

https://doi.org/10.1093/genetics/iyad019 Advance Access Publication Date: 10 February 2023 Investigation

Heterotrimeric G proteins regulate planarian regeneration and behavior

Jennifer E. Jenkins (D), Rachel H. Roberts-Galbraith (D)*

Department of Cellular Biology, University of Georgia, Athens, GA 30602, USA

*Corresponding author: Department of Cellular Biology, University of Georgia, 120 Cedar Street, Athens, GA 30602, USA. Email: robertsgalbraith@uga.edu

Abstract

G protein-coupled receptors play broad roles in development and stem cell biology, but few roles for G protein-coupled receptor signaling in complex tissue regeneration have been uncovered. Planarian flatworms robustly regenerate all tissues and provide a model with which to explore potential functions for G protein-coupled receptor signaling in somatic regeneration and pluripotent stem cell biology. As a first step toward exploring G protein-coupled receptor function in planarians, we investigated downstream signal transducers that work with G protein-coupled receptors, called heterotrimeric G proteins. Here, we characterized the complete heterotrimeric G protein complement in *Schmidtea mediterranea* for the first time and found that 7 heterotrimeric G protein subunits promote regeneration. We further characterized 2 subunits critical for regeneration, $G\alpha q1$ and $G\beta1$ -4a, finding that they promote the late phase of anterior polarity reestablishment, likely through anterior pole-produced Follistatin. Incidentally, we also found that 5 G protein subunits modulate planarian behavior. We further identified a putative serotonin receptor, gcr052, that we propose works with $G\alpha s2$ and $G\beta s2$ in planarian locomotion, demonstrating the utility of our strategy for identifying relevant G protein-coupled receptors. Our work provides foundational insight into roles of heterotrimeric G proteins in planarian biology and serves as a useful springboard toward broadening our understanding of G protein-coupled receptor signaling in adult tissue regeneration.

Keywords: planarian, regeneration, heterotrimeric G protein, GPCR, signaling, behavior, neurobiology, flatworm, Schmidtea

Introduction

G protein-coupled receptors (GPCRs) represent one of the largest, most highly conserved, and functionally diverse families of cell surface receptors (Anantharaman *et al.* 2011; Krishnan *et al.* 2012; Langenhan *et al.* 2015). GPCRs also comprise ~30% of drug targets, due to their broad involvement in cell signaling (Hopkins and Groom 2002; Wise *et al.* 2002; Garland 2013). GPCRs possess structures that include 7 transmembrane domains, extracellular domains for signal perception, and intracellular domains for interaction with signal transducers (Fig. 1a) (Pierce *et al.* 2002; Lagerström and Schiöth 2008). Canonically, activation of a GPCR initiates dissociation of a heterotrimeric G protein complex (Fig. 1a) into an α subunit and a β/γ subcomplex, both of which impact cellular function (Oldham and Hamm 2008; Smrcka 2008).

Importantly, GPCR signaling regulates wound response throughout the animal kingdom in organisms that include nematodes, fruit flies, and mammals (Ziegler et al. 2009; Doze and Perez 2013; Kiseleva et al. 2014; Zugasti et al. 2014; Choi et al. 2015; Guo et al. 2019; O'Connor et al. 2021). For example, the protease-activated receptor 1 (PAR1) GPCR promotes wound healing in murine skin by stimulating production of keratinocytes (Kiseleva et al. 2014). Downstream heterotrimeric G proteins also modulate regeneration. Ga class subunits from several families have been shown to promote or inhibit axon regeneration in

vertebrates (Bates and Meyer 1996; Li et al. 2016) and Caenorhabditis elegans (Shimizu and Hisamoto 2020). However, roles for GPCR pathways have not yet been explored in organisms that complete robust, whole-body regeneration. Studying GPCR signaling in highly regenerative models could reveal new roles for these pathways in regeneration of complex tissues.

Freshwater flatworms called planarians provide an appealing model for investigation of mechanisms underlying robust regeneration. After nearly any injury, planarians produce a blastema in which differentiating cells accumulate and mature to reconstruct missing structures (Baguna et al. 1989). Regeneration proceeds through key events that include wound detection (Wenemoser et al. 2012; Wurtzel et al. 2015), activation of pluripotent adult stem cells (Wagner et al. 2011; Raz et al. 2021), and polarity reestablishment (Witchley et al. 2013; Reddien 2018). Through these processes, planarians regenerate all tissues and complex organs de novo, including the brain. How planarian cells detect injury, reinterpret polarity axes, and mount the correct regenerative response after injury remain key areas of investigation. Because regeneration requires multifaceted, fine-tuned coordination of cellular responses after injury and because GPCR signaling functions in diverse aspects of cell biology and healing in other animals, we hypothesized that GPCR pathways play key roles in planarian regeneration that have yet to be discovered.

Currently, the genome of S. mediterranea is predicted to contain 566 GPCR-encoding genes (Zamanian et al. 2011; Saberi et al. 2016).

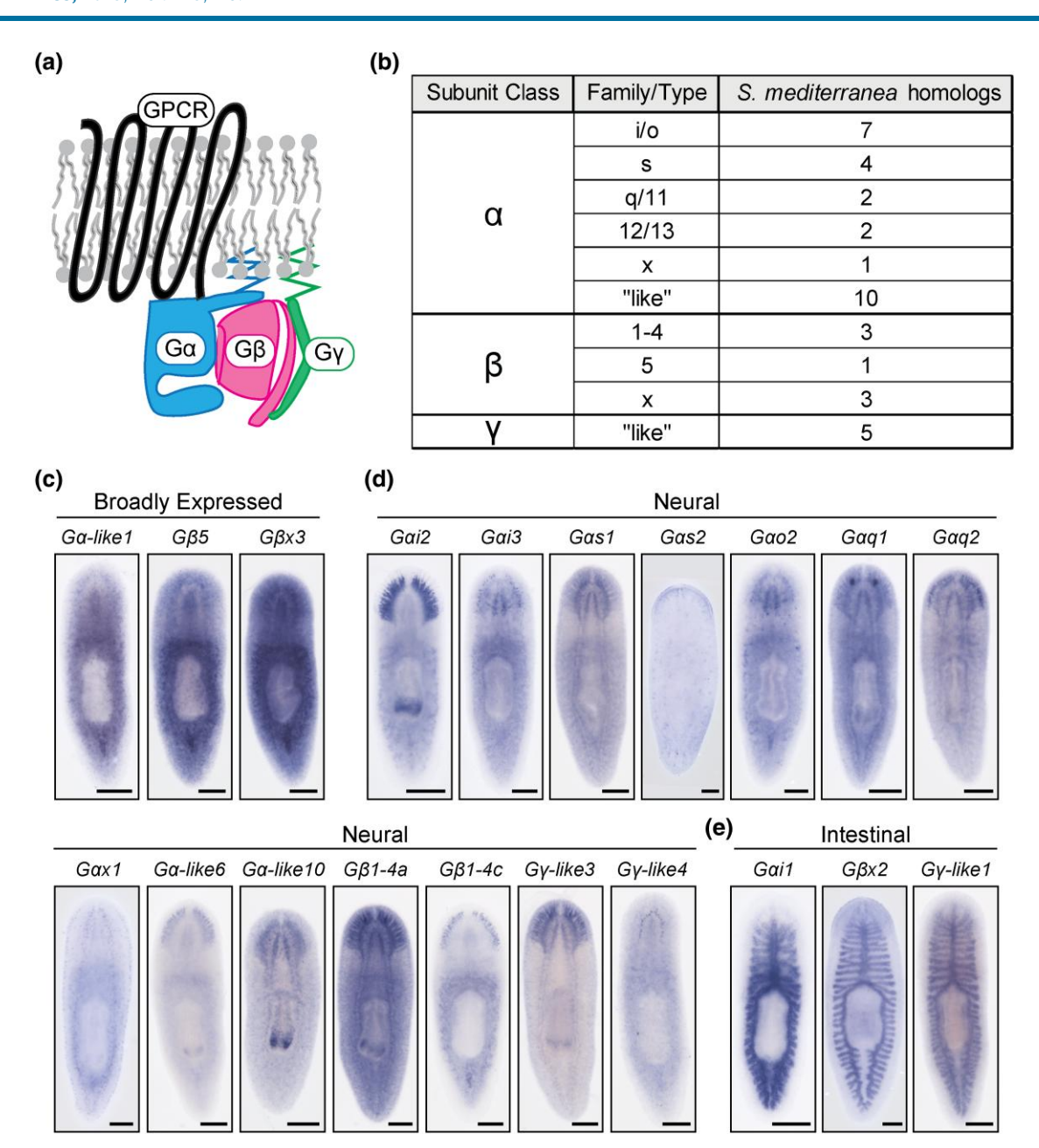


Fig. 1. Planarians possess diverse heterotrimeric G proteins. a) Graphical summary of a typical heterotrimeric G protein complex associated with a GPCR (top in the lipid bilayer). The heterotrimer is composed of $G\alpha$ (bottom left), $G\beta$ (bottom middle), and $G\gamma$ (bottom right) subunits that are activated upon ligand binding to the receptor. b) Table depicting S. *mediterranea* homologs for heterotrimeric G protein subunits. Representative images of G protein subunit expression patterns categorized by the most visually enriched tissue type into broad (c), neural (d), and intestinal (e) patterns. Scale bars = 200 μm. The anterior of the animals is oriented toward the top of the page in all figures.

Very few of these genes are functionally characterized, with the identified GPCRs promoting posterior identity, supporting planarian locomotion, coordinating germline differentiation and maintenance, facilitating reproductive system development and repair, or impacting eye regeneration (Zamanian 2011; Lozano 2015; Saberi et al. 2016; Pascual-Carreras et al. 2021). Characterization of planarian heterotrimeric G protein subunits is also limited. gpas is expressed in the brain branches and pharynx (Cebrià et al. 2002; Iglesias et al. 2011), while 4 other G protein subunit genes (gna-q, gna-o, gnb, and gnc) are highly expressed in photoreceptors (Lapan and Reddien 2012). Work among planarian species assessed function for a handful of specific GPCR/G protein pathways (Zamanian 2011; Zamanian et al. 2012; Chan et al. 2015; Chan et al. 2016). However, a comprehensive analysis of G protein

function could help indicate the extent to which GPCR pathways regulate tissue regeneration and help uncover new roles for GPCR pathways in planarians.

As an essential first step toward pursuing our hypothesis that GPCR signaling promotes regeneration, we characterized heterotrimeric G proteins in the planarian S. mediterranea. In this work, we identified and characterized 38 predicted heterotrimeric G protein subunit-encoding genes, which include highly conserved homologs of described vertebrate G protein families and divergent subunits. We show that 7 G protein subunit-encoding genes—Gas1, Gas2, Gaq1, Gaq2, Gao2, Ga-like6, and $G\beta1$ -4a—promote planarian regeneration. Two of the identified genes, Gaq1 and $G\beta1$ -4a, are essential for promoting the late phase of anterior–posterior axis reestablishment, likely by influencing production of

follistatin⁺ anterior pole cells. We also show that 5 genes—Gas1, Gas2, Gaq1, G β 1-4a, and G β x2—are required for planarian movement. To illustrate the utility of our G protein-centered approach to identifying key GPCRs, we further identified a GPCR-encoding gene, qcr052 (Saberi et al. 2016), as a potential partner of Gas2 and $G\beta x2$. Taken together, our results reveal new functions for heterotrimeric G protein signaling in the highly regenerative planarian model. Our data further provide a much-needed starting point for identifying GPCRs with roles in regeneration.

Materials and methods

Animal maintenance

Planarians from an asexual strain of the species S. mediterranea [CIW4 (Alvarado et al. 2002)] were kept in 1X Montjuïc salts [1.6-mM NaCl, 1-mM CaCl₂, 1-mM MgSO₄, 0.1-mM MgCl₂, 0.1-mM KCl, and 1.2-mM NaHCO₃ prepared in ELGA PURELAB (ELGA LabWater, Woodridge, IL) ultrapure water (Cebrià and Newmark 2005) at 18°C in the dark. Animals were fed beef liver puree weekly or biweekly. Animals were cut periodically to expand their numbers and generate properly sized (~2-5 mm) individuals for experiments. Animals were starved for a minimum of 1 week before experiments.

Gene identification

 $G\alpha$ subunit-like transcripts were mined using the guanine nucleotide-binding domain [PF00503 (Coleman et al. 1994)], GB subunit-like transcripts were mined using the WD40-repeatcontaining domain preceded by N-terminal alpha helix [IPR001632 (Wall et al. 1995)], and Gy subunit-like transcripts were mined using the GGL domain [PF00631 (Snow et al. 1998)]. Each relevant functional domain [from Pfam (El-Gebali et al. 2019) or InterPro (Mitchell et al. 2019)] was searched within the translated S. mediterranea transcript dataset dd_Smed_v6 (Brandl et al. 2016; Rozanski et al. 2019); then redundant transcripts were removed. To ensure the retrieved Gy subunit-like sequences were not regulators of G protein signaling (RGS) proteins, the absence of an RGS domain [PF00615 (Chen et al. 2001; Longenecker et al. 2001)] was confirmed (Supplementary Table 1).

Protein alignment and phylogenetic analysis

Amino acid sequences were predicted using the web-based translation tool Swiss ExPASy (Expert Protein Analysis System) Molecular Biology Server (Swiss Institute of Bioinformatics, University of Lausanne, Switzerland) (Gasteiger et al. 2003). Protein sequences were aligned to reference sequences from other animals (Supplementary Table 5) using Clustal Omega O (1.2.4) (Sievers and Higgins 2014), and secondary structures were predicted with ESPript3.0 (Robert and Gouet 2014), using wellcharacterized structure examples (PDB ID: 1GP2). Phylogeny was analyzed using www.phylogeny.fr (Dereeper et al. 2008). The "a la carte" option was selected with MUSCLE for alignment (Edgar 2004) and PhyML for construction of the phylogenetic tree (Guindon et al. 2010). For the PhyML analysis, 100 bootstrap replicates were performed, and the WAG model of amino acid substitution was applied.

Molecular cloning

For genes of interest, primers were designed using Primer3 (Rozen and Skaletsky 1999) to amplify an ~700-bp region of the corresponding gene from asexual S. mediterranea cDNA (Supplementary Table 6). PCR products were cloned into the vector, pJC53.2 (Collins et al. 2010) using standard molecular biology protocols.

RNA interference (RNAi) experiments

The dsRNA was transcribed in vitro from PCR products amplified from pJC53.2 using standard molecular methods (Collins et al. 2010; Rouhana et al. 2013). Concentration of dsRNA was determined using either a NanoPhotometer NP80 (Implen, Munich, Germany) or by band intensity after gel electrophoresis. For a typical experiment, 10-12 animals were fed 1-3-µg dsRNA mixed in ~30-µL food (beef liver paste, 4:1 liver:salts mixture), and 1-µL green food dye was added to verify that the animals ate. The mixture was doubled for larger experiments. Negative control worms were fed dsRNA matching green fluorescent protein (GFP) or bacterial genes [chloramphenicol resistance gene (CmR) and toxin CcdB (ccdB)]. Animals were kept in 60–100-mm Petri dishes. After eating, the animals were washed and transferred to fresh dishes, and salts were supplemented with 1:1000 gentamicin sulfate [50-mg/mL stock (Gemini Bio, West Sacramento, CA)]. Animals were fed dsRNA ~once per week for 3 total feedings [more feedings given in long-term RNAi experiments (Fig. 2; Supplementary Fig. 6)] and then were processed. Live images during experiments were obtained using a Zeiss Axiocam 506 color camera mounted on a Zeiss Axio Zoom.V16 microscope (ZEISS Microscopy, Jena, Germany). Live images and video were also captured on an iPhone 6 and/or SE and processed in iMovie (Apple Inc., Cupertino, California).

Behavior assays

For the flipping assay (Fig. 2b-c), live recordings were captured for up to 5 min after each animal was put on its dorsal side. We observed how long it took each animal to flip to its ventral side. For locomotion studies (Fig. 2; Supplementary Fig. 3), animals were recorded in 13 x 13-mm/square grid dishes (VWR International, Radnor, PA) for at least 15 min. Velocity was quantified for 8-12 individual animals, while they showed forward movement over at least a 40-s timespan. Distance was tracked using BioTracker (Mönck et al. 2018); then velocity was calculated for intervals of 4 s. Average velocities were determined from the values of 11 successive intervals. For negative phototaxis assays (Supplementary Fig. 3D), animals were put in 13 x 13-mm/square grid dishes (VWR International, Radnor, PA) with lids half-covered with black electrical tape. This produced an uncovered/light side and covered/dark side of the dish. Animals were placed in the farleft corner of the uncovered region and then recorded for at least 10 min. For each 60-s interval, the number of animals visible in the uncovered region was documented.

In situ hybridization (ISH)

Single-stranded antisense riboprobes were transcribed with digoxigenin (Dig-11-UTP) (Sigma-Aldrich, St. Louis, MO) using standard molecular methods (Collins et al. 2010). Animals were fixed, hybridized with riboprobes, and stained as previously described (King and Newmark 2013), with the following modifications: animals were killed in a 10% N-acetyl cysteine solution and treated with a 2-µg/ml Proteinase K solution. Regenerating animals were treated with the Proteinase K/postfixation steps (as opposed to a boiling step). After the hybridization step, 56°C washes were as follows: one 20-min wash in wash hyb [25% formamide, 3.5X SSC (0.15-M NaCl, 0.015-M Na citrate), 0.1% Triton X-100, and pH 7.0], three 20-min 2X SSCx (2X SSC and 0.1% Triton X-100) washes, and four 20-min 0.2X SSCx (0.2X SSC and 0.1% Triton X-100) washes. We also replaced MABT with TNTx

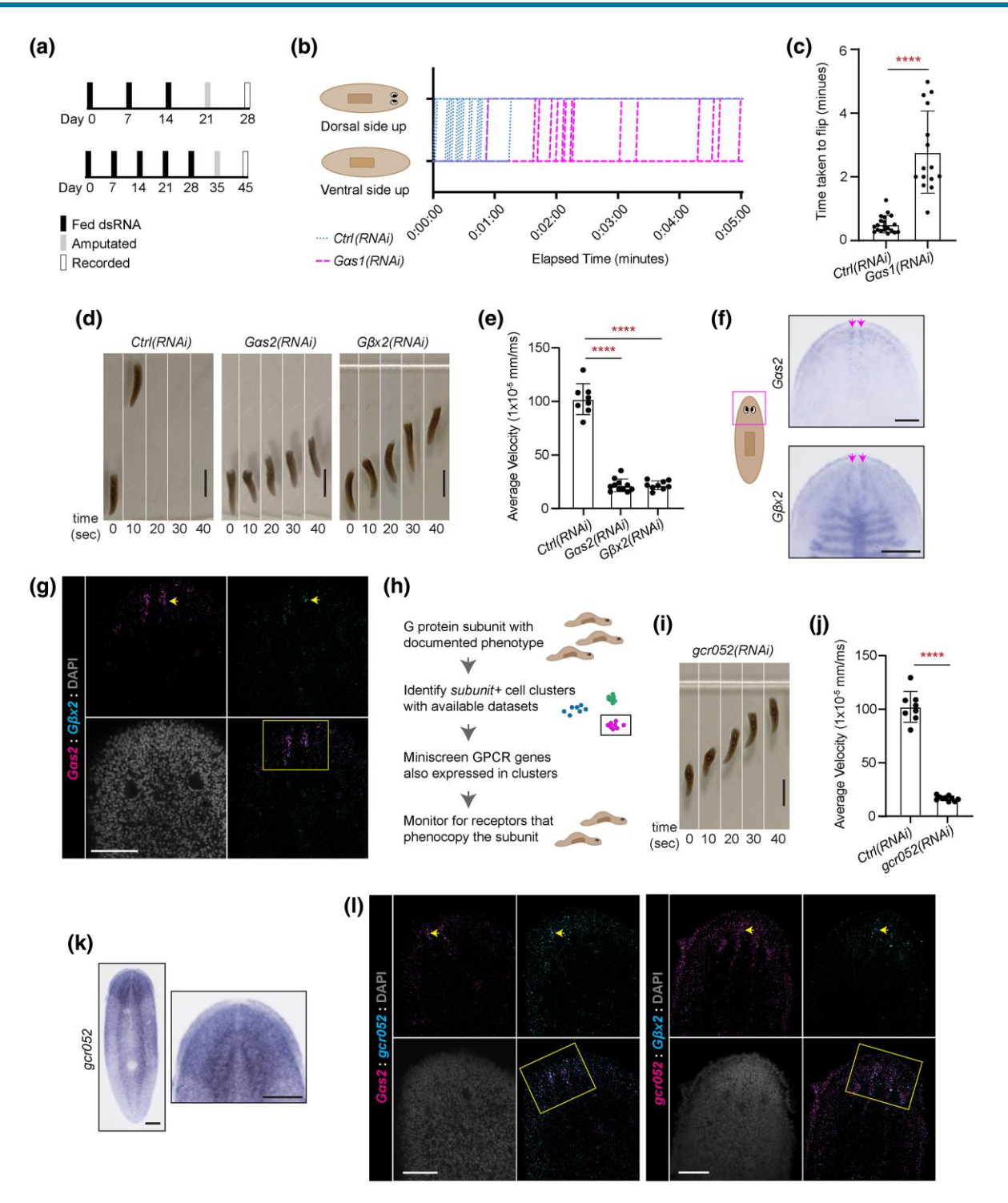


Fig. 2. Planarian heterotrimeric G proteins and GCR052 promote animal movement. a) RNAi paradigms used during initial regeneration screens (top) and follow-up, longer-term experiments (bottom). Data from b-c resulted from the top paradigm, and data from d-e and i-j resulted from the bottom paradigm. b) Flip assay used to document paralysis in Gas1(RNAi) animals. The graph includes flipping data for 20 animals per RNAi condition. c) Bar graph showing times taken for animals to flip over to a correct ventral-down posture (excluding 5 nonflipping Gas1(RNAi) animals), displayed as mean and standard deviation. Differences were analyzed with unpaired t-test with Welch's correction. **** = P value ≤ 0.0001. d) Image stills from videos capturing locomotion displayed by regenerating control, Gas2(RNAi), and G\(\beta x2(RNAi) \) animals 10 dpa. e) Results from quantification of average velocity over a 40-s timespan in regenerating control, Gas2(RNAi), and $G\beta x2(RNAi)$ animals, displayed as mean and standard deviation. f) Images of Gas2 and $G\beta x2$ zoomed colorimetric ISH showing the clusters of cells at the anterior tip of the animals, indicated with arrowheads. g) Gas2 and GBx2 dFISH images of the head region. Arrowhead indicates an example of a cell enriched with both transcripts. The box indicates the region of interest where the anterior clusters are found. h) Graphical scheme showing the method used to identify candidate GPCRs for G protein subunits with documented phenotypes. i) Image stills from videos capturing locomotion displayed by regenerating gcr052 (RNAi) animals. j) Results from quantification of average velocity over a 40-s timespan in intact control and gcr052(RNAi) animals, displayed as mean and standard deviation. Data displayed in i-j are from the same experiment as shown in d-e. Differences in average velocities were analyzed with Brown-Forsythe and Welch ANOVA with multiple comparisons. ****= P value ≤ 0.0001. k) Images showing the expression pattern of gcr052 through colorimetric ISH. l) gcr052 dFISH images with Gas2 or GBx2 in the head region. The box indicates the region of interest where the anterior clusters are found. Arrowheads indicate an example of a cell enriched with both transcripts. Scale bars in d and i = 2 mm. Scale bars in f and $d = 200 \mu m$. Scale bars in g and $l = 100 \mu m$.

(0.1-M Tris pH 7.5, 0.15-M NaCl, and 0.3% Triton X-100). After antibody incubation, animals were washed in TNTx for 5 min (1 wash), 10 min (1 wash), and 20 min (6 washes). The fixation step after sample development was omitted. Other key reagents include antidigoxigenin conjugated with an alkaline phosphatase (anti-Dig-AP 1:2000 dilution), nitro blue tetrazolium (NBT), and 5-bromo-4-chloro-3'-indolylphosphate (BCIP) (all Sigma-Aldrich, St. Louis, MO). Animals were mounted in 80% glycerol and imaged with a Zeiss Axiocam 506 color camera mounted on a Zeiss Axio Zoom. V16 microscope (ZEISS Microscopy, Jena, Germany).

Fluorescent ISH (FISH)

Single-stranded antisense riboprobes were synthesized with digoxigenin (Dig-11-UTP) (Sigma-Aldrich, St. Louis, MO), fluorescein isothiocyanate (FITC-12-UTP) (Roche, Basel, Switzerland), or 2,4-dinitrophenol (DNP) (PerkinElmer, Inc., Waltham, MA) using standard molecular methods (Collins et al. 2010). Riboprobes were detected using anti-Dig-POD (1:1000; Sigma-Aldrich, St. Louis, MO), anti-FITC-POD (1:1000; Sigma-Aldrich, St. Louis, MO), or anti-DNP-HRP (1:3000; Vector Laboratories, Newark, CA). Tyramide conjugate signal amplification was performed as previously described (King and Newmark 2013). The final incubation was with DAPI (10 µg/ml) (1:1000; Thermo Fisher Scientific, Waltham, MA). Animals were mounted in VECTASHIELD (Vector Labs, Burlingame, CA) for imaging.

Immunofluorescence (IF)

Immunofluorescence was adapted from existing protocols (Forsthoefel et al. 2014; Ross et al. 2015). Planarians were killed in 2% HCl for 5 min with alternating 1-min incubations on ice and gently inverting at room temperature. The HCl step was followed by three 5-min washes in PBS (phosphate-buffered saline: 137-mM NaCl, 2.7-mM KCl, 10-mM Na₂HPO₄, 2-mM KH₂PO₄, pH 7.4) at room temperature. Animals were then fixed for 15 min in 4% formaldehyde solution in PBS and then shaken in PBSTx (PBS and 0.3% Triton X-100) for 10 min 3 times at room temperature. The animals were bleached under light overnight in 6% H2O2 in PBSTx. Bleaching was followed by two 10-min PBSTx washes at room temperature. Animals were then blocked [PBSTx and 1% bovine serum albumin (Jackson ImmunoResearch Laboratories, Inc., West Grove, PA)] for at least 4 h. Blocking solution was replaced with a solution containing primary antibody anti-phospho-histone H3 (Ser10) [1:1600 (Cell Signaling Technology, Danvers, MA)] to mark cells in the process of mitosis and were incubated gently shaking at 4°C overnight. The next day animals were incubated in PBSTx at room temperature 8 times for 30 min. Then animals were incubated in blocking solution for 1 h. Blocking solution was replaced with a solution containing the secondary antibody, goat-antimouse IgG + IgM-horseradish peroxidase [1:1000 (Sigma-Aldrich, St. Louis, MO)], and animals were shaken gently at 4°C overnight. Afterward, animals were washed for 30 min 8 times in PBSTx at room temperature. The samples were then shaken for 30 min at room temperature in PBSTi (PBSTx and 10-mM imidazole) wrapped in foil (foil remained until mounting). The samples were then developed for 5 min through tyramide signal amplification (TSA reaction) using FITC-tyramide (1:1000 in PBSTi and 0.015% H_2O_2). The samples were then shaken at room temperature in PBSTx 3 times for 10 min and then 2 times for 30 min. The final incubation was in DAPI solution (0.5 µg/ml in PBSTx) overnight at 4°C. Samples were then mounted in VECTASHIELD (Vector Labs, Newark, CA) for imaging.

Confocal image acquisition

Confocal images were obtained for FISH and IF samples using Zen Black 2.3 SP1 software on a Zeiss LSM 710 AXIO Observer Z1 inverted microscope or Zeiss 880 Axio Imager Z2 microscope (ZEISS Microscopy, Jena, Germany). The details for FISH images are as follows: Fig. 2g and 2l are single slice images using a 20x objective (numerical aperture [NA] 0.8); the head region images in Fig. 3h are max intensity projections of 10 z-sections (9.72-µm sections) taken with a 10x objective (NA 0.3); the zoomed eyespot images in Fig. 3h are single slices captured with a 40x objective (NA 1.4); Supplementary Fig. 6a are max intensity projections of 12 z-sections (1-µm sections) taken with a 20x objective (NA 0.8); and Supplementary Fig. 6b are single slices taken with a 20x objective (NA 0.8). For H3P IF, images of 4 tiles and ~30 z-sections (1-µm sections) capturing the anterior half of the animals were taken with a 10x objective (NA 0.3). For post-processing, tiles were stitched with Imaris (Oxford Instruments, Abingdon, United Kingdom) or FIJI (FIJI is just ImageJ, Schindelin et al. 2012) software.

Image quantification

For regeneration assays, areas of the brains (Fig. 3; 6 and Supplementary Fig. 4; 8) or blastemas (Supplementary Fig. 4) were measured from fixed sample images by tracing the structures with FIJI imaging software (Schindelin et al. 2012) and normalized as described previously (Roberts-Galbraith et al. 2016) (Supplementary Table 4). Brain measurements were traced around the outer boundary of the brain, encompassing the entire structure including the brain branches. For growth assays (Supplementary Fig. 6), animal lengths were measured from live images in FIJI (Schindelin et al. 2012). Data were statistically analyzed and visualized using Prism GraphPad Version 7.0 software (GraphPad Software, San Diego, CA). Specific tests employed are found in the corresponding figure legends.

For H3P analysis, Imaris software (Oxford Instruments, Abingdon, United Kingdom) was used for quantification of H3P+ cells in the body volume of the anterior half of 4-5 animals per RNAi treatment. The spots function of the software was employed to detect green cells. After automated counting, spots were manually checked and adjusted. The surface function was employed to measure the body volume captured in each z-stack. Mitoses/mm³ was calculated from the total number of H3P+ cells in a given volume.

Quantitative reverse transcription polymerase chain reaction

RNA was extracted from animals using TRIzol Reagent (Thermo Fisher Scientific, Waltham, MA) as per the manufacturer's protocol (Liu and Rink 2018). Samples were treated with RQ1 RNase-free DNase (Promega Corporation, Madison, WI) for 15 min at 37°C. cDNA was synthesized from RNA using an iScript kit (Bio-Rad, Hercules, CA). Quantitative reverse transcription polymerase chain reaction (RT-qPCR) reactions were completed using SYBR Green PCR Master Mix (Bio-Rad, Hercules, CA) in a QuantStudio® 3 real-time PCR system (Applied Biosystems, Foster City, CA). Primers were generated in Primer3 (Rozen and Skaletsky 1999) and targeted sequences ~100 bp in length (Supplementary Table 6). RT-qPCR primers were designed to match a region of the transcripts not included in dsRNA constructs using Benchling software (Benchling, San Francisco, CA). Transcript abundance for genes of interest was normalized using the control gene, β tubulin (Collins et al. 2010). Experiments were performed in biological and technical triplicate (n = 12 animals

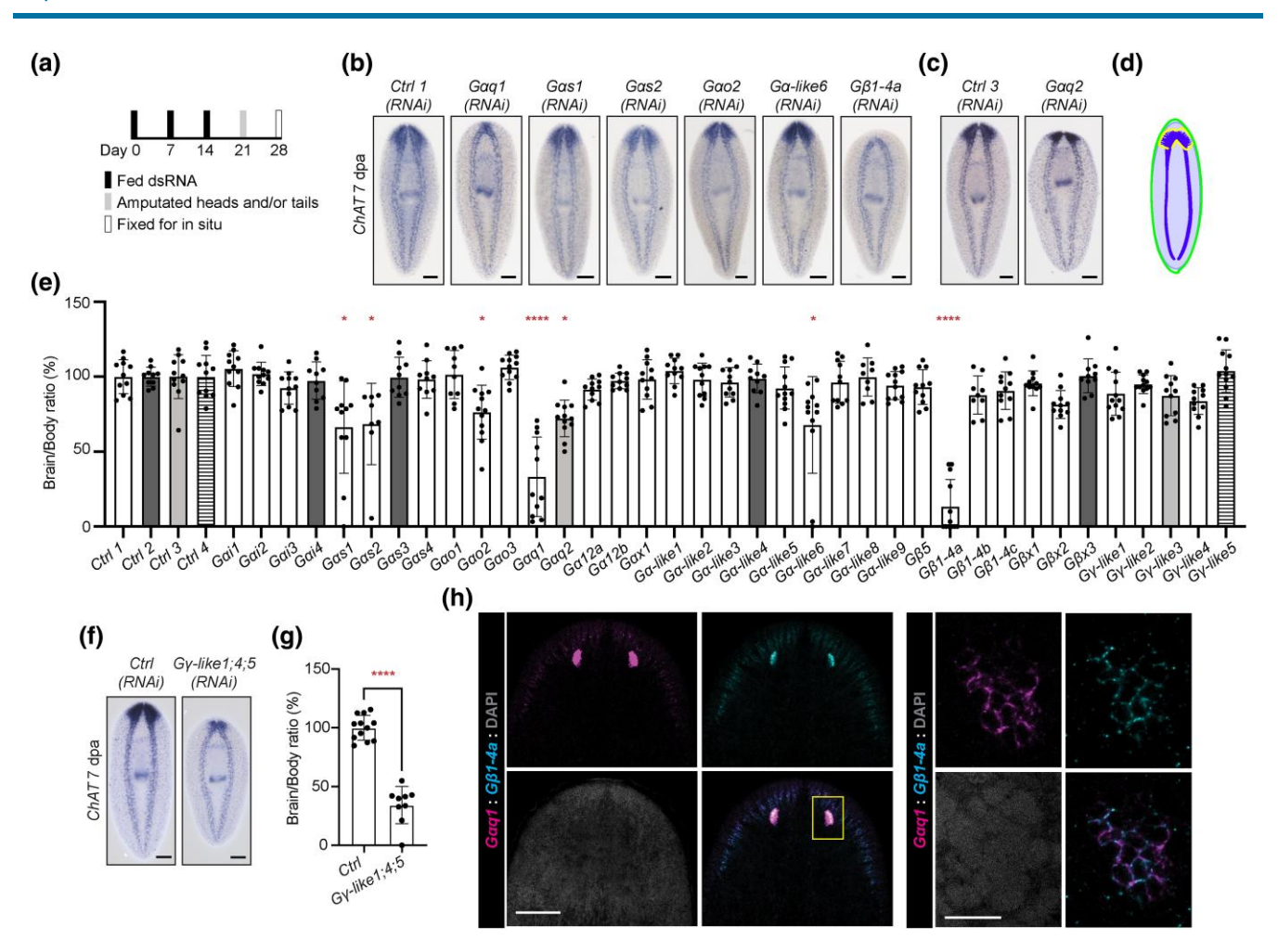


Fig. 3. Specific planarian heterotrimeric G protein genes promote brain regeneration. a) RNAi paradigm used for initial regeneration screens. b and c) Representative images showing animals treated with RNAi targeting genes that reduced brain regeneration along with corresponding controls. d) Visual schematic displaying our method for brain regeneration quantification. From ChATISH images, the area of the brain and body for each animal are used to calculate brain/body ratios (Roberts-Galbraith et al. 2016). e) Bar graph of data from quantification of brain/body ratios after RNAi, displaying mean and standard deviation. Bars are color coded to match samples to controls from the same experiment. Differences were analyzed using Brown-Forsythe and Welch ANOVA. *= P value ≤ 0.05. **** = P value ≤ 0.0001. f) Representative images showing brain regeneration in control and combinatorial Gy-like1, Gy-like4, and Gy-like5 (RNAi) animals. g) Bar graph of quantified brain/body ratios in Gy-like combinatorial RNAi, displayed as mean and standard deviation. Differences were analyzed using unpaired t-test. **** = P value \leq 0.0001. h) Gaq1 and $G\beta1$ -4a dFISH images focusing on the head. The box indicates the region shown in the next, zoomed image of the eyespot, validating coexpression. Scales in b, c, and f and the head region image in h = 200 μ m. Scale in the eyespot image of h = 20 μ m.

per biological replicate). Data were statistically analyzed and visualized using Prism GraphPad Version 7.0 software (GraphPad Software, San Diego, CA).

Results

Identification of the planarian G protein subunit repertoire

To better understand G protein-coupled receptor signaling in planarians, we identified 38 G protein subunit homologs (26 G α subunits, 7 G β subunits, and 5 G γ subunits) in S. mediterranea transcriptomes based on the presence of key domains (Brandl et al. 2016; Rozanski et al. 2019) (Fig. 1b, Supplementary Table 1). This list included all 5 previously identified planarian G protein subunit genes (Cebrià et al. 2002; Iglesias et al. 2011; Lapan and Reddien 2012). Both numbers and proportions of subunits are consistent with those found in other animals, including humans (Syrovatkina et al. 2016), C. elegans (Jansen et al. 1999), and Drosophila (Malpe et al. 2020). These results suggest that planarians utilize a typical repertoire of heterotrimeric G protein subunits.

We next classified planarian heterotrimeric subunit homologs into families using phylogenetic analysis. We classified 7 Gαi/o homologs, 4 Gas homologs, 2 Gaq/11 homologs, 2 Ga12/13 homologs, 3 G\u03bb1-4 subgroup homologs, and 1 G\u03bb5 homolog (Fig. 1b; Supplementary File S1; S2). One $G\alpha$ homolog and 3 $G\beta$ homologs contained all functional domains (Supplementary File S1) but did not cluster with a specific family (Suppplementary File S2). We therefore designated these genes as " $G\alpha x$ " or " $G\beta x$ " (Fig. 1b). Additionally, 10 $G\alpha$ class homologs retrieved in our search were truncated, preventing accurate classification (Supplementary File S3). We designated these genes $G\alpha$ -like (Fig. 1b). Lastly, due to the divergent nature of Gy homologs, we were unable to classify them into families, so we designated them as "Gy-like" (Fig. 1b; Supplementary File S1; S2). Our phylogenetic analysis suggests that the $G\alpha$ class homolog gpas (Cebrià et al. 2002; Iglesias et al. 2011) was previously misclassified, and the name $G\alpha i2$ more accurately represents this subunit's classification.

After defining the S. mediterranea heterotrimeric G protein complement, we next sought to characterize the expression patterns of these genes, to potentially provide insight into tissue-specific roles and possible heterotrimer combinations. We observed broad expression for 9 G protein subunit homologs (Fig. 1c; Supplementary Fig. 1). However, many subunits showed tissuespecific enrichment in the nervous system (Fig. 1d; Supplementary Fig. 1) or the intestine (Fig. 1e). Lastly, we detected no expression pattern for 2 subunits through ISH (Supplementary Fig. 1). In addition to our observations, we determined that 32 of the 38 subunits are expressed within stem cells based on available transcriptomic resources (Labbé et al. 2012; Fincher et al. 2018; Plass et al. 2018; Zeng et al. 2018) (Supplementary Table 1). Our results suggest that S. mediterranea heterotrimeric G proteins likely function in many different tissue types, including stem cells and a diverse set of neural cell types.

Elucidation of roles for heterotrimeric G proteins in planarian behavior

We next performed, to our knowledge, the first comprehensive investigation into roles for planarian heterotrimeric G proteins. We completed an RNAi screen by feeding dsRNA and assessing behavioral and regenerative phenotypes (Fig. 2a). We evaluated the penetrance of RNAi for a sampling of 5 genes in these screens using RT-qPCR and observed knockdown efficiency ranging from 92 to 98% (Supplementary Fig. 2a). Specificity of knockdown was examined with the two subunits with the most similar DNA sequence, $G\beta$ 1-4a and $G\beta$ 1-4b (58% identity, with stretches of up to 20 identical base pairs). We note that we did observe some degree of cross-reactivity for the dsRNA of these subunits at the level of RT-qPCR but did not see overlap in phenotypes after RNAi (Supplementary Fig. 2b).

Though our ultimate focus was on regeneration, during our screens, we incidentally observed that knockdown of 5 G protein subunit-encoding genes caused behavioral phenotypes. The strongest behavior we documented was reduced movement and paralysis in Gαs1(RNAi) animals, which was most clear when animals were placed on their dorsal sides (Supplementary Video S1). All control animals righted themselves after being placed on their dorsal side, taking an average of 27.35 s (Fig. 2b-c). In contrast, 5 of 20 $G\alpha$ s1(RNAi) animals failed to flip onto their ventral side within 5 min. The remaining Gas1 (RNAi) animals took an average of 168 s to flip (Fig. 2b-c). These results indicate that Gas1 is required for the righting response and gross movement in planarians. Although we saw reduced movement prior to amputation, the paralysis and flipping phenotypes were enhanced after amputation or long-term RNAi, which may suggest that the movement phenotype results from loss of a slow-turnover cell type (Supplementary Table 2).

Inhibition of any of 4 genes—Gas2, G β x2, G β 1-4a, and Gaq1—resulted in decreased gliding movement, which leads to "inching" behavior (Glazer et al. 2010). The quickest effects were seen following RNAi of $G\alpha$ s2 or $G\beta$ x2. We first documented the inching after amputation (Fig. 2d), but the phenotype was nearly identical in intact worms (Fig. S3a; Supplementary Table 2; Supplementary Videos 2-3). Movement defects in $G\alpha$ s2(RNAi) and $G\beta$ x2(RNAi) animals resulted in reduced distance traveled over time (Fig. 2e; Supplementary Fig. 3b). Gaq1(RNAi) animals also appeared to move slower than controls in short-term RNAi paradigms, and amputation marginally increased this phenotype (Supplementary Table 2). After long-term RNAi, Gaq1(RNAi) animals displayed labored movement (Supplementary Fig. 3c; Supplementary Video 4). G\u03b31-4a(RNAi) animals alternated between inching and gliding, most perceptibly after amputation or long-term RNAi (Supplementary Fig. 3c; Supplementary Table 2; Supplementary Video 4). An assay documenting negative

phototaxis in these animals also demonstrated slow movement to a dark area of a dish, with the strongest effects resulting from perturbation of $G\beta x2$ (Supplementary Fig. 3d). Finally, we also note that $G\alpha q1(RNAi)$, $G\beta 1-4a(RNAi)$, $G\alpha s2(RNAi)$, and $G\beta x2(RNAi)$ animals spent a noticeable amount of time raising and turning their heads, which may be indicative of additional sensory or movement dysfunction.

Locomotion of Gαs2(RNAi) and Gβx2(RNAi) animals was indistinguishable, which led us to hypothesize that $G\alpha s2$ and $G\beta x2$ might be operating in the same cells. We noted that $G\alpha$ s2 is expressed in a head margin pattern consistent with putative peripheral sensory neurons (Ross et al. 2018) (Fig. 1d, Fig. 2f). $G\beta x2$ is expressed in a similar pattern but also in cells of the intestine (Fig. 1e, Fig. 2f). We further validated the coexpression of $G\alpha$ s2 and $G\beta x2$ in cells at the tip of the head through FISH (Fig. 2g). The colocalization of $G\alpha s2$ and $G\beta x2$ transcripts supports the hypothesis that they could potentially work in the same cells.

Our goal in focusing on heterotrimeric G proteins was to uncover roles for GPCRs. As proof-of-principle, we next sought to identify the GPCR that works with $G\alpha s2$ and $G\beta x2$. We identified and screened 8 GPCR-encoding genes enriched in the same cell clusters as $G\alpha$ s2 or $G\beta$ x2 in available single cell sequencing datasets (Fincher et al. 2018; Plass et al. 2018) (Fig. 2h; Supplementary Table 3). Using this method, we identified a putative serotonin receptor, qcr052 [the homolog of DtSER-1 (Zamanian et al. 2012), S7.1R (Chan et al. 2015, 2016), and Smed-ser85 (Zamanian 2011) in planarian literature], for which knockdown caused inching indistinguishable from that displayed by $G\alpha$ s2(RNAi) and $G\beta$ x2(RNAi) animals (Fig. 2i-j; Supplementary Videos 2-3; Supplementary Fig. 3a-b).

gcr052 is expressed broadly throughout the CNS (Fig. 2k). Using FISH, we detected coexpression of gcr052 with G α s2 and G β x2 in many cells, including clusters at the anterior (Fig. 21). While targeting $G\alpha$ s2, $G\beta$ x2, and/or gcr052 in combination did not noticeably exacerbate the phenotype (Supplementary Fig. 3e-f; Supplementary Video S5), some GPCR research indicates that loss of one component can prevent the assembly of the receptor/ trimer complex (Smrcka 2008; Dupré et al. 2009). We thus hypothesize that G α s2 and G β x2 act downstream of the GCR052 receptor to support gliding motion.

In summary, our results show that 5 planarian heterotrimeric G proteins are essential for normal animal movement. Additionally, our identification of GCR052 provides proof-of-principle that the heterotrimeric G proteins characterized in this work can accelerate planarian GPCR research.

Planarian heterotrimeric G proteins function in regeneration

Over the course of our functional analysis, we knocked down each G protein subunit and assessed the degree of brain regeneration after amputation (Fig. 3a-e; Supplementary Table 4), because brain size is a highly robust way of detecting regeneration defects (Roberts-Galbraith et al. 2016). After screening 37 of the 38 predicted subunit genes, we found 7 genes for which RNAi caused significant reduction in brain regeneration (Fig. 3b-e). Of these candidates, RNAi targeting Gas1, Gas2, Gao2, Gaq2, or Ga-like6 produced modest effects (Fig. 3b–e). RNAi targeting $G\alpha q1$ or $G\beta 1$ -4a caused a strong reduction of brain regeneration (Fig. 3b-e). Of these genes, knockdown of 3 candidate subunits, $G\alpha$ s1, $G\alpha$ q1, or $G\beta$ 1-4 α , also caused reduction in tail regeneration (Supplementary Fig. 4a-c). These results show that multiple $G\alpha$ class and one $G\beta$ class subunit play roles in planarian regeneration.

Interestingly, we detected no significant regeneration phenotypes after RNAi targeting individual Gγ subunit genes (Fig. 3e). To account for potential functional redundancy among Gγ subunits, we observed brain regeneration after combinatorial RNAi targeting all identified Gy class subunit genes (Supplementary Fig. 4d). Indeed, targeting these genes concurrently produced a significant ~46% reduction in regenerated brain size (Supplementary Fig. 4d). Furthermore, RNAi of Gy-like1, Gy-like4, and Gy-like5 together caused a severe reduction in brain regeneration (Fig. 3f-g). These results indicate that Gy subunits are likely functionally redundant and have cooperative roles in regeneration.

Due to the strong roles for $G\alpha q1$ and $G\beta 1$ -4a in regeneration, we sought to further identify the cell types that express $G\alpha q1$ and $G\beta$ 1-4a and determine whether these genes are expressed in overlapping cells. Based on the colorimetric ISH expression patterns, the transcripts of $G\alpha q1$ and $G\beta 1$ -4a appear to both be particularly enriched in the central nervous system and eyespots (Fig. 1d). Additionally, based on published sequencing datasets, these genes are also detected in muscle and at low levels in stem cells (Supplementary Table 1). We confirmed expression of Gaq1 and $G\beta$ 1-4a in the brain branches and eyespots through FISH (Fig. 3h). Additionally, due to the highly enriched expression in the eyespots, we took a closer look at these cells and saw that $G\alpha q1$ and $G\beta 1$ -4a transcripts indeed colocalize (Fig. 3h). Although we require biochemical analyses to prove functional pairing, these results show that $G\alpha q1$ and $G\beta 1-4a$ are expressed in overlapping cell populations.

Additionally, we considered that $G\alpha q1$ or $G\beta 1$ -4a could impact regeneration by affecting the timing of tissue regrowth. To determine whether the phenotypes we saw were due to delays in regeneration, we observed brain regeneration at 14 days postamputation (dpa) in knockdown animals. Gaq1 (RNAi) and $G\beta1$ -4a(RNAi) animals showed partial recovery of regenerated brain size with additional time (Supplementary Fig. 4e). However, we note that the distribution of brain regeneration is not the same in Gaq1(RNAi) and $G\beta$ 1-4a(RNAi) animals. A small proportion of $G\alpha$ 91(RNAi) animals failed to initiate any regenerative response, and while the rest of the animals regenerated the expected brain size, brain morphology appeared more collapsed toward the midline relative to control brains (Supplementary Fig. 4e). In contrast, all $G\beta$ 1-4a(RNAi) animals regenerated a reduced, but otherwise normal, bilobed brain structure (Supplementary Fig. 4e). Our results at 14 dpa support the notion that $G\beta$ 1-4a promotes the speed of brain regeneration, whereas Gaq1 shows a more complex role in brain regeneration including initiation of regenerative response and proper morphology of the mature CNS.

Through these studies, we find that multiple heterotrimeric G proteins promote regeneration, with $G\alpha q1$ and $G\beta 1$ -4a playing especially critical roles. Further, although we saw overlap in roles for regeneration and behavior after perturbation of some genes (Gαs1, Gαs2, Gαq1, and Gβ1-4a), some genes specifically impact regeneration (Gao2, Gaq2, and Ga-like6) or behavior (G β x2) (Figs. 2 and 3, and Supplementary Table 2).

*Gβ*1-4*a* promotes mitotic response after amputation and long-term survival

Our next goal was to understand why $G\alpha q1$ and $G\beta 1$ -4a are critical for regeneration. We first considered whether $G\alpha q1$ and $G\beta 1$ -4a affect initial response to wounding. We examined the expression of $G\alpha q1$ and $G\beta 1-4a$ after injury. Indeed, we found that $G\alpha q1$ and $G\beta$ 1-4a are upregulated at the amputation site at both 6 h postamputation (hpa) and 3 dpa (Supplementary Fig. 5a). Planarians initiate a molecular wound response program during this time that includes upregulation of genes like follistatin, jun-1, inhibin, and wnt1 (Wenemoser et al. 2012; Wurtzel et al. 2015). We determined that $G\alpha q1(RNAi)$ and $G\beta 1-4a(RNAi)$ animals expressed wound-induced genes normally at 6 hpa (Supplementary Fig. 5b-c). The only significant difference we observed was a mild increase in follistatin transcripts in Gaq1(RNAi) animals, detected through RT-qPCR (Supplementary Fig. 5c). These results suggest that while $G\alpha q1$ and $G\beta 1$ -4a are upregulated during regeneration, they are dispensable for early injury response.

Next, we investigated whether the regeneration defects observed after Gaq1(RNAi) or $G\beta1-4a(RNAi)$ result from perturbed stem cell maintenance or differentiation. We looked at expression of a stem cell marker [Smedwi-1 (Reddien et al. 2005)] and epidermal progenitor markers [proq-1 and AGAT-1 (Eisenhoffer et al. 2008; Tu et al. 2015)] after head regeneration. We did not see depletion of stem cell or progenitor markers through ISH (Fig. 4a-c). However, transcript abundance of Smedwi-1 showed modest or mild reduction through RT-qPCR after RNAi of $G\alpha q1$ or $G\beta 1-4a$, respectively (Fig. 4d).

We also examined mitotic activity of stem cells in Gaq1 (RNAi) and $G\beta$ 1-4a(RNAi) animals. Planarian stem cells divide at a regular rate in intact animals, and after amputation two primary waves of mitosis occur: one at ~6 hpa that is body-wide and one at ~48 hpa that is localized to the amputation site (Baguna et al. 1989; Wenemoser and Reddien 2010). To investigate the rates of stem cell division in $G\alpha q1(RNAi)$ and $G\beta 1-4a(RNAi)$ animals, we performed an antibody stain for a histone modification associated with mitosis (phospho-histone-H3-Ser10) (Hendzel et al. 1997; Newmark and Sánchez Alvarado 2000). We detected a significant decrease in proliferative cells in $G\beta$ 1-4a(RNAi) animals at 48 hpa, but otherwise the mitotic activity in $G\alpha q1$ (RNAi) and $G\beta$ 1-4a(RNAi) animals appeared comparable to controls (Fig. 4e– f). We also found that $G\beta$ 1-4a is not strongly coexpressed with Smedwi-1 in intact or regenerating animals, but we did see $G\beta1-4a^+$ and Smedwi-1⁺ cells near one another in regenerating tissue (Supplementary Fig. 6a-b), suggesting that any effect of Gβ1-4a signaling on stem cells might be noncell autonomous. We conclude that $G\alpha q1$ and $G\beta 1-4a$ may play subtle roles in stem cell maintenance, differentiation, or division, but that these defects are likely insufficient to explain the severe regenerative phenotypes seen in RNAi animals.

Finally, we asked whether the roles of $G\alpha q1$ and $G\beta 1$ -4a were exclusive to regeneration or whether either gene also functioned during homeostasis. We performed longer term RNAi and measured animal growth and survival over time (Supplementary Fig. 6c). $G\beta$ 1-4a(RNAi) animals ceased growth after day 21 and we halted the growth measurements of Gαq1(RNAi) animals at that time point because they began to fission (Supplementary Fig. 6d). Long-term RNAi targeting $G\beta$ 1-4a was lethal, with animals showing head lysis and dying near day 40 (Supplementary Fig. 6ef). We also noted postural changes without change in viability in Gaq1 (RNAi) animals, suggesting that Gaq1 promotes head regeneration but is not required for head maintenance (Supplementary Fig. 6e-f). Intriguingly, Smedwi-1+ cells remained abundant at later timepoints of RNAi (Supplementary Fig. 6g-h), suggesting that the stem cells are maintained even as $G\beta1-4a(RNAi)$ animals begin to lyse.

To summarize, our data indicate that $G\alpha q1$ is essential for regeneration but not strictly required for wound response induction, mitosis, or stem cell maintenance. Long-term inhibition of $G\beta$ 1-4a is lethal, but other than modestly promoting the late wave of mitotic response after amputation, we did not detect strong impacts of $G\beta$ 1-4 α perturbation on stem cell regulation.

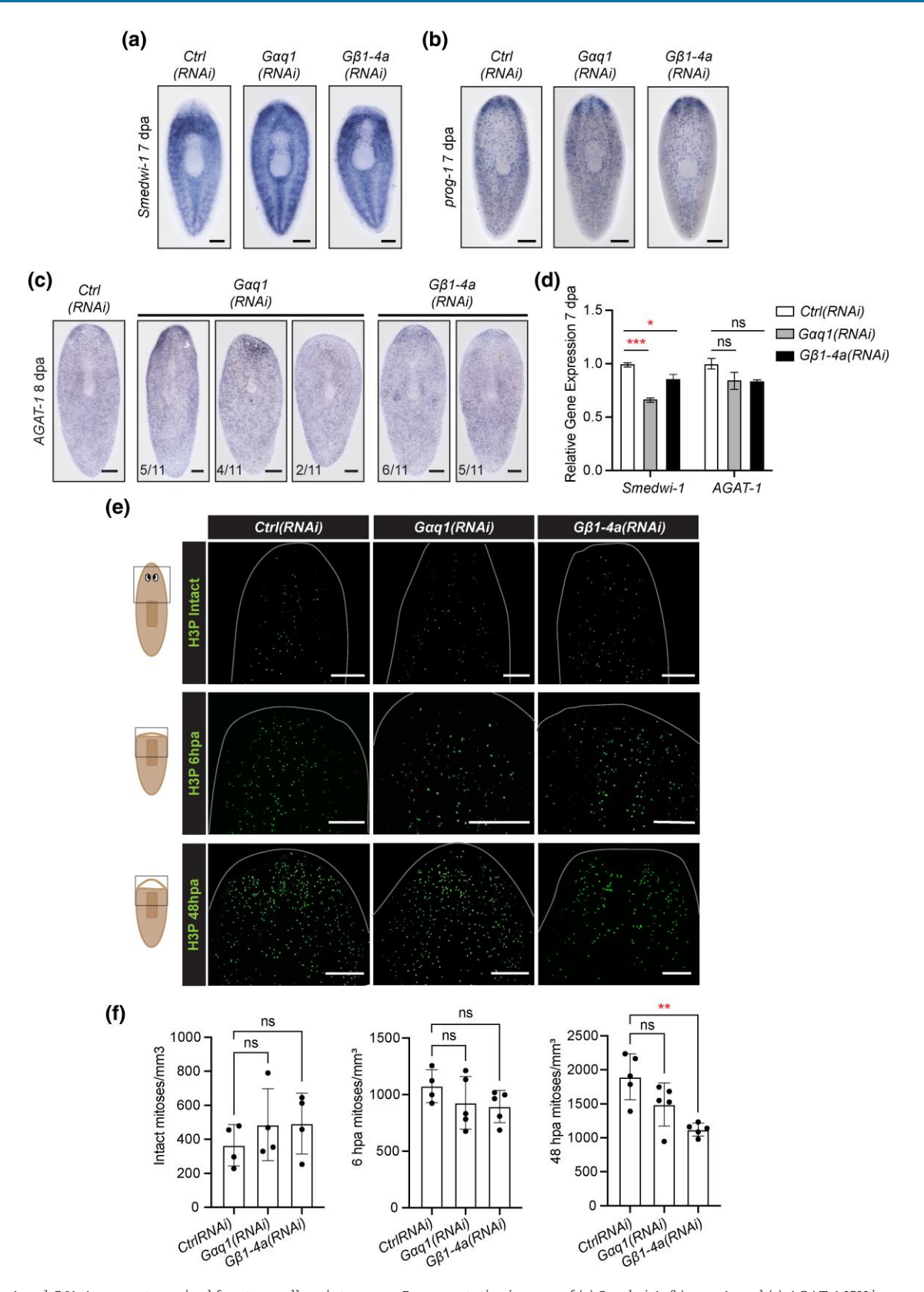


Fig. 4. Gaq1 and G\u00bb1-4a are not required for stem cell maintenance. Representative images of (a) Smedwi-1, (b) proq-1, and (c) AGAT-1 ISH in regenerating animals after RNAi targeting Gaq1 and $G\beta1$ -4a. d) Relative transcript abundance of stem cell markers, measured by RT-qPCR. Differences were analyzed with one-way ANOVA with multiple comparisons. Error bars represent standard error. *= P value \leq 0.005. *** = P value \leq 0.0005. e) Representative images of proliferative cell detection (anti-H3P) at the anterior region of intact, 6-h regenerating and 48-h regenerating RNAi animals. f) Results from quantification of H3P+ cells detected in the anterior region of the animals at each timepoint, displayed as mean and standard deviation. Differences were analyzed with Brown-Forsythe and Welch ANOVA with multiple comparisons. ** = P value \leq 0.01. Scale bars = 200 μ m.

Importantly, several results indicate key differences in function for $G\alpha q1$ and $G\beta 1-4a$, despite the two genes having similarly important roles in regeneration. Because the impacts we saw for both subunits in stem cell biology were mild, we sought to examine influences of $G\alpha q1$ and $G\beta 1$ -4a on other physiological processes that contribute to regeneration.

$G\alpha q1$ and $G\beta 1-4a$ support the late phase of anterior-posterior polarity reestablishment

Early in planarian regeneration, tissues reorganize to pattern body axes using conserved developmental signaling pathways [e.g. Wnt/β-catenin (Gurley et al. 2008; Iglesias et al. 2008; Petersen and Reddien 2008)]. We next considered whether regeneration failures after $G\alpha q1(RNAi)$ or $G\beta 1-4a(RNAi)$ occur due to abnormal body polarity. During the early phase of polarity reestablishment, the remaining tissue determines which end of the animal is anterior and which is posterior (Fig. 5a) [reviewed in (Owlarn and Bartscherer 2016)]. To determine whether Gaq1(RNAi) and Gβ1-4a(RNAi) animals correctly complete the initial anterior–posterior decision, we examined notum and wnt1 expression 18 hpa (Fig. 5b). notum expression resumed normally at the anterior in $G\alpha q1(RNAi)$ and $G\beta 1-4a(RNAi)$ animals (Fig. 5c). $G\alpha q1(RNAi)$ animals also expressed bipolar wnt1, but over half of $G\beta$ 1-4a(RNAi) animals displayed posterior-enriched expression of wnt1 (Fig. 5c). These results suggest that $G\alpha q1$ is not involved in early polarity decisions, but G\beta 1-4a might affect anterior wound-induced wnt1 expression.

After re-initiation of axial polarity, anterior and posterior poles form at the distal ends of the planarian body (Fig. 5a). To determine whether pole formation was disrupted in Gaq1(RNAi) and $G\beta$ 1-4a(RNAi) animals, we analyzed notum and wnt1 expression at 3 dpa (Fig. 5b). 50% of $G\alpha q1$ (RNAi) animals and all $G\beta$ 1-4a(RNAi) animals lacked anterior notum expression (Fig. 5d). Additionally, $G\alpha q1$ (RNAi) animals displayed an asymmetric wnt1 pattern or absent wnt1 in the posterior domain, and Gβ1-4a(RNAi) animals regenerated with a broadened and/or asymmetrical domain of wnt1 expression (Fig. 5d). Our results indicate that $G\alpha q1$ and $G\beta 1$ -4a impact pole formation at both anterior and posterior ends of the animal.

During the late phase of polarity reestablishment, anterior and posterior poles further coalesce and mature (Fig. 5a). To investigate whether $G\alpha q1$ and $G\beta 1-4a$ support the maturation of the key polarity domains, we examined expression of notum and another posterior marker, wnt11-2 (Gurley et al. 2008), in knockdown animals at 7 dpa (Fig. 5b). We observed a lack of notum staining at the anterior pole in \sim 25% of $G\alpha q1$ (RNAi) animals (Fig. 5e), and we confirmed this pattern by using a second pole marker, sFRP-1 (Gurley et al. 2008; Petersen and Reddien 2008) (Supplementary Fig. 7a). Posterior pole maturation was also disrupted in ~33% of Gaq1(RNAi) animals, which displayed broader and more diffuse wnt11-2 expression (Fig. 5e). All Gβ1-4a(RNAi) animals recovered anterior notum expression by 7 dpa, although the domains appeared less consolidated than in control animals, which could signify slower maturation (Fig. 5e, Supplementary Fig. 7a). The formation of an anterior pole domain at a slower pace is consistent with our previous results suggesting that $G\beta$ 1-4a largely affects the speed of head regeneration rather than ultimate success (Supplementary Fig. 4e). Strikingly, most $G\beta$ 1-4a(RNAi) animals expressed posterior wnt11-2 asymmetrically, with staining on either side of the animal's midline (Fig. 5e). Notched tails were also commonly seen after $G\beta$ 1-4a(RNAi) (Supplementary Fig. 4c), though our data did not support the presence of a

secondary anterior domain, as has been seen after other RNAi treatments (Supplementary Fig. 7b-c) (Cloutier et al. 2021).

Taken together, we conclude that $G\beta$ 1-4a supports the speed of anterior pole reestablishment and promotes proper midline placement of the posterior pole. Our data also support a role for Gaq1 in promoting robust anterior pole formation, though this phenotype was limited to a minority of animals. Interestingly, while both $G\alpha q1$ and $G\beta 1$ -4a function during regeneration and influence anterior-posterior polarity, the precise phenotypes seen after RNAi of $G\alpha q1$ and $G\beta 1$ -4a are distinct.

Gaq1 promotes head regeneration through production and activity of follistatin⁺ anterior pole

The anterior pole is established and maintained through two mutually dependent signaling proteins, Notum and Follistatin (Petersen and Reddien 2011; Gaviño et al. 2013; Roberts-Galbraith and Newmark 2013). notum and follistatin encode key extracellular inhibitors of posterior-promoting Wnt and Activin pathways, respectively (Nakamura et al. 1990; Kakugawa et al. 2015). We noted several similarities between the phenotypes caused by follistatin(RNAi) and those caused by $G\alpha q1$ (RNAi) or $G\beta 1$ -4a(RNAi). Similarities include strong impacts on head and brain regeneration; reduced or delayed notum expression in the regenerating head; unaffected expression of early wound response genes; and subtle impacts on stem cells (Gaviño et al. 2013; Roberts-Galbraith and Newmark 2013; Tewari et al. 2018).

Based on phenotypic similarities, we sought to determine whether RNAi of Gαq1 or Gβ1-4a impacts follistatin expression during regeneration (Fig. 6a). We detected no change in follistatin expression at 12 hpa after perturbation of $G\alpha q1$ or $G\beta 1-4a$ (Fig. 6b). We similarly saw equivalent or higher follistatin transcripts 6 hpa through RT-qPCR (Supplementary Fig. 5c). These results indicate that regeneration failure in $G\alpha q1$ (RNAi) and $G\beta 1$ -4a(RNAi) animals is not correlated with a reduction of wound-induced follistatin expression.

To determine whether $G\alpha q1$ and $G\beta 1$ -4a support follistatin expression in the anterior pole, we examined follistatin expression during pole formation (Fig. 6a). At 3 dpa, most $G\alpha q1$ (RNAi) and all $G\beta$ 1-4a(RNAi) animals had absent follistatin expression at the anterior pole (Fig. 6c). At 7 dpa, \sim 36% of $G\alpha g1$ (RNAi) animals still lacked follistatin+ anterior pole cells (Fig. 6d). However, all $G\beta$ 1-4a(RNAi) animals established follistatin⁺ pole cells by 7 dpa (Fig. 6d), reflecting a similar delay in anterior pole formation seen with other markers (Fig. 5 and Supplementary Fig. 7).

Both notum and follistatin expression in anterior pole cell progenitors relies on a key transcription factor, encoded by foxD (Roberts-Galbraith and Newmark 2013; Scimone et al. 2014; Vogg et al. 2014). To investigate whether Gaq1 could modulate follistatin through FoxD, we examined foxD expression following Gaq1 knockdown. Indeed, anterior foxD expression was absent in 50% of Gaq1(RNAi) animals at 3 dpa and ~36% of animals at 7 dpa (Supplementary Fig. 7d-e). We confirmed this significant reduction of foxD expression through RT-qPCR (Supplementary Fig. 7f). $G\beta$ 1-4a(RNAi) animals displayed absent foxD anterior pole expression 3 dpa and most animals resumed foxD expression by 7 dpa (Supplementary Fig. 7d-e). Thus, our data suggest that impacts on follistatin expression could be mediated by foxD. Alternatively, the lack of these anterior pole markers could result from a failure to produce and/or specify anterior pole progenitors, resulting in fewer pole cells.

Previous work characterizing the Follistatin/Activin and Notum/Wnt pathways determined that reduction of the antagonistic posterior-promoting ligands rescued head regeneration

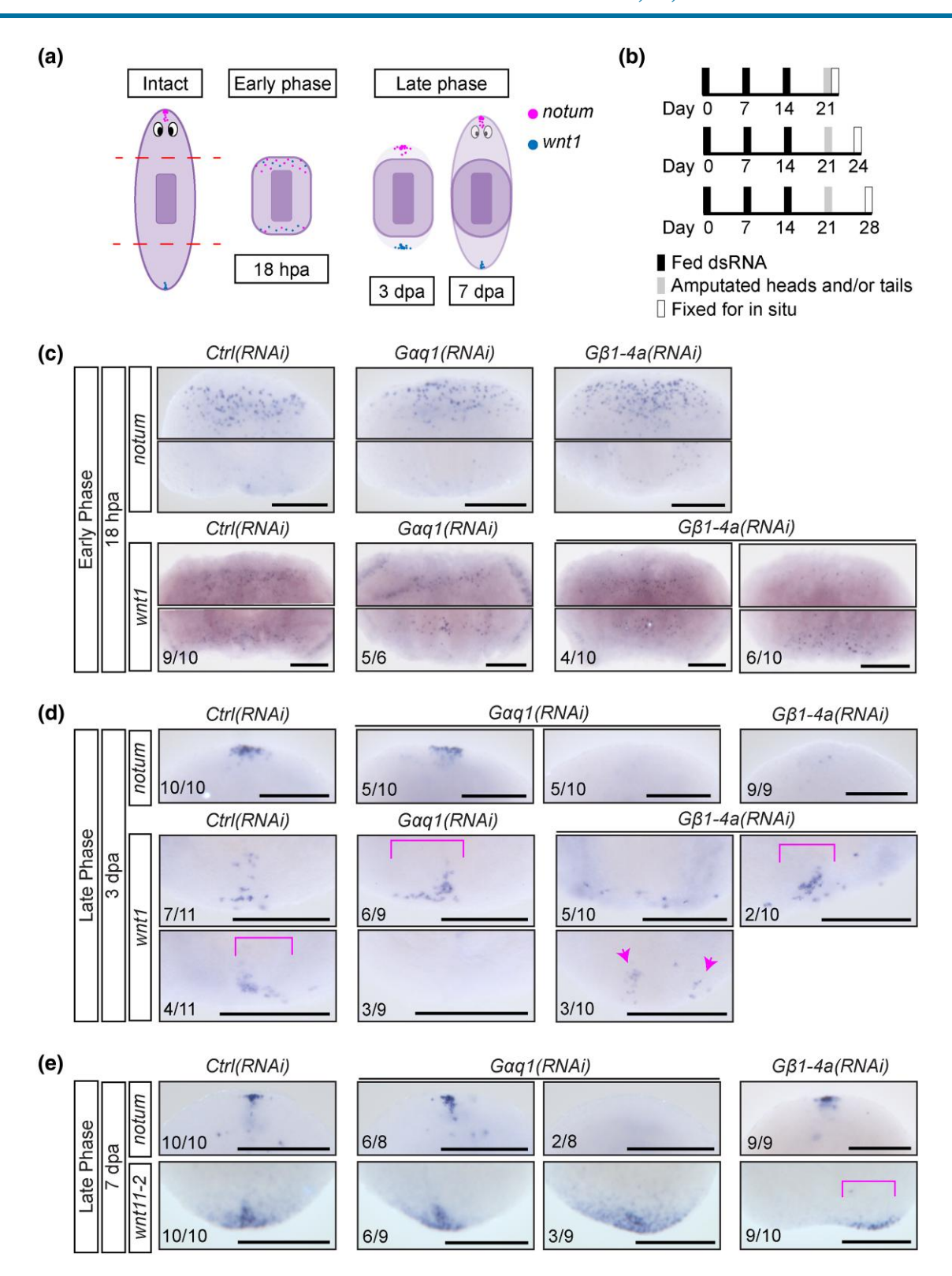


Fig. 5. Gaq1 and G\u00bb1-4a support the late phase of anterior and posterior pole regeneration. a) Graphic summary depicting phases of polarity reestablishment after head and tail amputation, as summarized in (Owlarn and Bartscherer 2016). b) RNAi paradigms for 18 hpa (top), 3 dpa (middle), and 7 dpa (bottom). The following images are zoomed to focus on the regenerating head or tail blastemas for each stage. Representative images of anterior notum, and posterior wnt1 or wnt11-2 expression at (c) 18 hpa, (d) 3 dpa, and (e) 7 dpa of heads (pointing upward) and/or tails (pointing downward). Brackets denote nonmedial expression domains. Arrowheads indicate multiple expression domains. Scale bars = 200 µm.

(Petersen and Reddien 2011; Gaviño et al. 2013; Roberts-Galbraith and Newmark 2013). The similarities between Gaq1(RNAi) and follistatin(RNAi) phenotypes and the impact of Gaq1(RNAi) on follistatin expression led us to hypothesize that $G\alpha q1$ functions to promote Follistatin signaling from the pole. To test this hypothesis, we performed RNAi targeting Gaq1 with activin(RNAi),

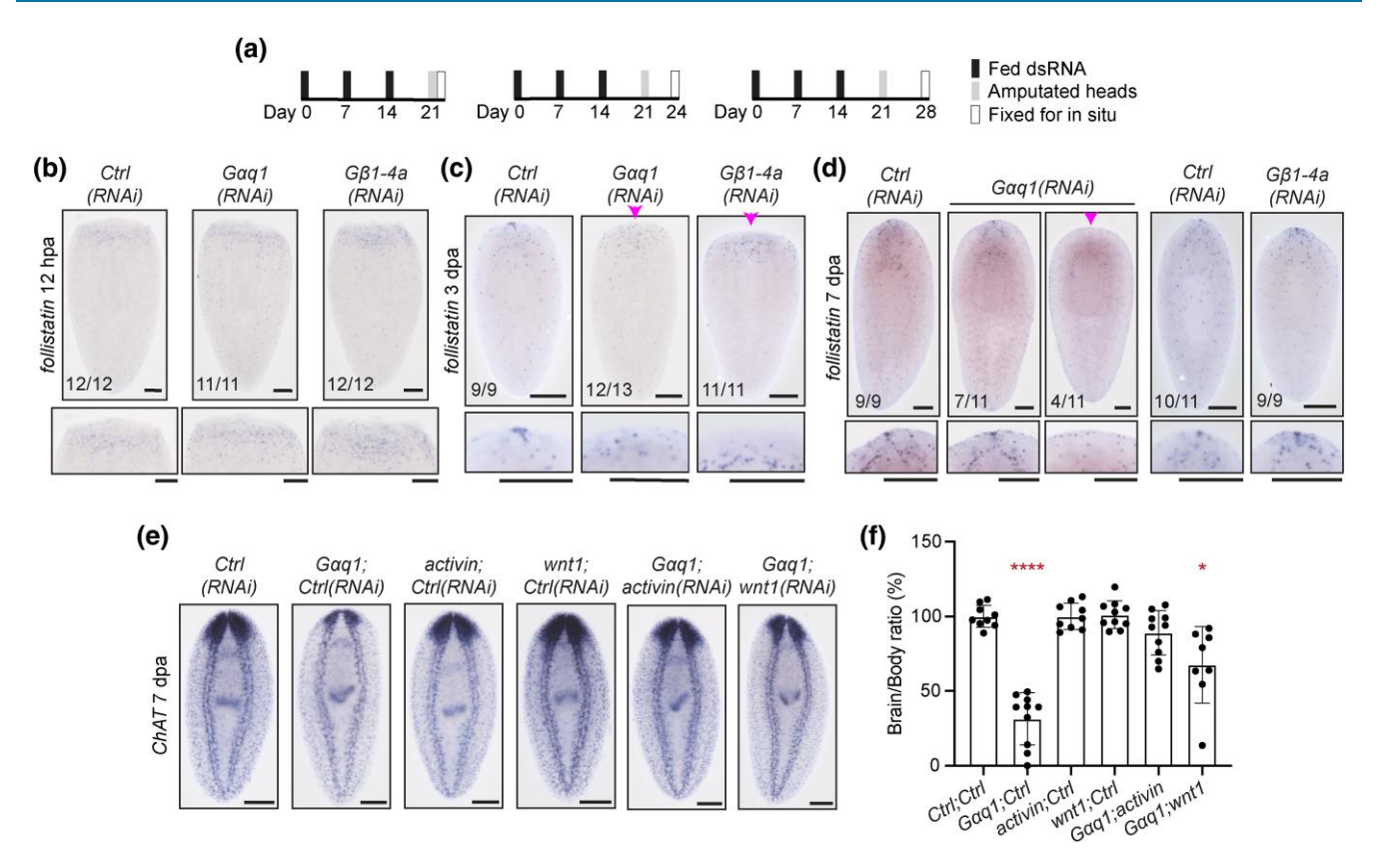


Fig. 6. Gaq1 supports head regeneration through production of follistatin⁺ anterior pole cells. a) RNAi paradigms used for data presented at 12 hpa (left), 3 dpa (middle), and 7 dpa (right). Representative images of follistatin expression at (b) 12 hpa, (c) 3 dpa, and (d) 7 dpa in Gaq1(RNAi) and $G\beta1-4a(RNAi)$ animals. Arrowheads indicate absent anterior pole expression domain. Insets show close-up images of the animals above. e) Representative images showing ChAT expression from rescue experiments 7 dpa. f) Bar graph showing results from quantification of brain/body ratios in rescue experiments, displayed as mean and standard deviation. Differences were analyzed using Brown–Forsythe and Welch ANOVA with multiple comparisons. *= P value \leq 0.05 and **** = P value \leq 0.0001. Scale bars = 200 μ m.

wnt1(RNAi), or bmp4(RNAi) (a TGF-β ligand that impacts dorsoventral polarity) (Reddien et al. 2007; Gaviño et al. 2013; Roberts-Galbraith and Newmark 2013; Tewari et al. 2018). activin(RNAi) significantly rescued Gaq1(RNAi)-induced brain regeneration defects (Fig. 6e-f; Supplementary Fig. 8a-e). wnt1(RNAi) also partially rescued Gaq1(RNAi) (Fig. 6e-f; Supplementary Fig. 8a-e). As expected, bmp4(RNAi) failed to rescue regeneration in Gaq1(RNAi) animals (Supplementary Fig. 8a-b). Our results were also confirmed in a second experiment that showed equally strong Gaq1 knockdown efficiency in double RNAi conditions (Supplementary Fig. 8c-e). Incidentally, though we primarily focused on a functional connection between Gaq1 and Follistatin, we also found that activin inhibition modestly restored brain regeneration in GB1-4a(RNAi) animals (Supplementary Fig. 8f-g). We conclude that $G\alpha q1$ function specifically supports Follistatin signaling from the anterior pole during head regeneration.

Discussion

The vast number of GPCRs hinders progress in understanding the function of this fascinating receptor family in planarian regeneration and stem cell biology. In this work, we take a step toward investigating planarian GPCR signaling by identifying and functionally characterizing the heterotrimeric G protein subunit complement in behavior and regeneration. We characterized 38 heterotrimeric G protein homologs, of which 23 were conserved enough to categorize. Through our functional screens, we

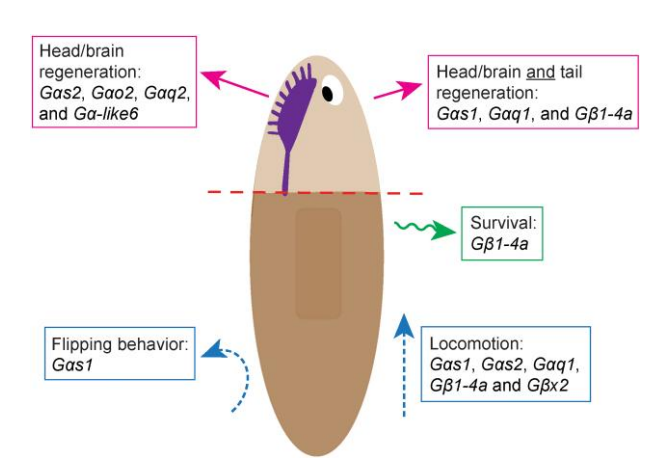


Fig. 7. Planarian heterotrimeric G proteins play diverse roles in regeneration, physiology, and behavior. Graphical summary of roles described in this work for heterotrimeric G proteins in S. *mediterranea*.

identified 5 subunit genes required for proper planarian movement (Fig. 7). Using these data as a starting point and relying on single cell sequencing data, we identified a putative serotonin receptor (GCR052) that could function with Gas2 and G β x2 in movement. Through our brain regeneration screen, we identified 7 genes with roles in regeneration, with Gaq1 and G β 1-4a having especially significant effects (Fig. 7). We determined that Gaq1 and

 $G\beta$ 1-4a promote successful regeneration and establishment speed of the anterior pole, respectively. Our findings indicate new pathways active in planarian regeneration and behavior and support the hypothesis that GPCR signaling is likely to be involved in key molecular events that drive and coordinate planarian regeneration.

Due to the functionally overlapping, but nonidentical effects of $G\alpha q1$ or $G\beta 1-4a$, we reason that these subunits could be activated downstream of a common GPCR but stimulate different downstream pathways to support tissue regeneration (Tang and Gilman 1991; Inglese et al. 1995; Brock et al. 2003). This model is supported by coexpression of Gaq1 and $G\beta1$ -4a through FISH and in single cell sequencing data (Fincher et al. 2018) (Fig. 3h; Supplementary Table 1 and 3). Additionally, we show through RT-qPCR that while targeting $G\beta$ 1-4a does not impact expression of $G\alpha q1$, expression of $G\beta 1-4a$ is significantly reduced in Gaq1(RNAi) animals (Supplementary Fig. 2c). We also demonstrated phenotypes for $G\beta1$ -4a(RNAi) but not $G\beta1$ -4b(RNAi), despite some cross-targeting of dsRNA (Supplementary Fig. 2). This indicates that the relationships between G protein subunits could involve additional redundancy or regulatory elements.

Gaq1 provides a putative connection between planarian GPCR signaling and defined polarity axes

phenotypic similarities between Gaq1(RNAi) and follistatin(RNAi) animals and the ability to rescue phenotypes via activin double knockdown indicate that the G α q1 protein likely cooperates with Follistatin during regeneration. Our results suggest that Gaq1 could function upstream to promote follistatin expression at the anterior pole. How Gαq1 promotes follistatin expression and whether this results from a failure to specify early anterior pole progenitors or a failure to turn on key gene networks in differentiating anterior pole cells remain to be determined. Alternatively, Activin signals belong to the transforming growth factor-β (TGF-β) family, and recent work describes the potential for GPCRs to modulate TGF- β pathways through transactivation (Burch et al. 2012; Hinck et al. 2016; Schafer and Blaxall 2017). Therefore, $G\alpha q1$ could potentially influence the Activin/ Follistatin axis through a noncanonical mechanism. Further exploring relationships between Gaq1 and pathway components will help define the nature of the $G\alpha q1$ /Follistatin cooperation.

Additionally, because $G\alpha q1$ (RNAi) animals displayed functional wound-induced follistatin expression, our results also support the notion that follistatin expression from the anterior pole is specifically needed to drive successful head regeneration (Gaviño et al. 2013; Roberts-Galbraith and Newmark 2013; Tewari et al. 2018). Therefore, results from future work with Gaq1 could inform the nature of anterior identity establishment. Potential roles for Gaq1 (and GPCRs) in modulating the Activin pathway and promoting polarity reestablishment will require further investigation.

The relationship between $G\alpha s2$, $G\beta x2$, and gcr052suggests complexity of serotonin's role in planarian locomotion

In addition to characterizing planarian heterotrimeric G proteins with roles in regeneration, this work also contributes to knowledge of mechanisms governing planarian movement. The current model for planarian gliding is that serotonergic neurons directly innervate ventral epidermal cells and coordinate the beating of motile cilia (Currie and Pearson 2013; März et al. 2013). Furthermore, experiments with mianserin, a pharmacological inhibitor of serotonin receptors, also implicated GPCRs in cilia

coordination in S. mediterranea (Kuang et al. 2002; Currie and Pearson 2013). In this work, we identify 2 G protein subunits ($G\alpha$ s2 and $G\beta$ x2) that similarly affect locomotion in S. mediterranea (Fig. 2). We further identified gcr052 (Saberi et al. 2016), which encodes a putative serotonin GPCR, as a potential specific mediator of gliding motion. Homologs of the receptor gcr052 have well documented roles in movement among planarian species, with coupling validation to Gαs protein family subunits [receptor referred to in literature as DtSER-1 (Zamanian et al. 2012), S7.1R (Chan et al. 2015, 2016), and Smed-ser85 (Zamanian 2011)]. We identified the receptor through our study of G proteins, displaying the usefulness of our pipeline method.

Further supporting the notion that Gas2 and GBx2 operate together and downstream of GCR052, we identified cells that are enriched with $G\alpha s2/G\beta x2$, $G\alpha s2/gcr052$, and $G\beta x2/gcr052$ through FISH (Fig. 2). These cells are patterned similarly to cells of the soxB1-2+ dorsal ciliated stripes of sensory neurons in the peripheral nervous system (Ross et al. 2018). While these cells were the most identifiable localization of all 3 transcripts, we note that additional cell types also appeared enriched for one or more of these genes. For example, we also observed high levels of gcr052 in putative epidermal cells at the periphery of the animal, potentially supporting the model that serotonin directly influences ciliary coordination on the epidermal cells via this receptor (Fig. 21). However, $G\alpha s2$ and $G\beta x2$ transcripts were not highly enriched in these cells, suggesting that serotonin signaling to other cells, such as the putative neurons described here, may also be important for planarian locomotion. Future work further characterizing the specific cells in which $G\alpha s2$, $G\beta x2$, and gcr052 operate in vivo, along with detailed documentation of how these genes affect planarian motile cilia, could elucidate the mechanisms regulating neural control of ciliabased gliding.

Furthermore, additional assays may reveal new roles of heterotrimeric G proteins in behavior and sensation. G proteins act in diverse biological processes, such as sensation, in other animals (Jones and Reed 1989; Yarfitz and Hurley 1994; Wong et al. 1996), and 8 planarian G protein subunits show expression enrichment in sensory structures called the brain branches (Agata et al. 1998; Okamoto et al. 2005), further supporting this notion (Fig. 1; Supplementary Fig. 9). Using the G protein group as a primary screening strategy may be a beneficial starting point for future study of GPCRs in planarian sensory neurobiology or other aspects of planarian physiology.

Planarian heterotrimeric G proteins can suggest candidate receptors for future planarian GPCR research

Because GPCRs represent one of the largest receptor families in many organisms, including humans (Fredriksson et al. 2003) and planarians (Zamanian et al. 2011; Saberi et al. 2016), approaches to accelerate identification of relevant GPCRs for a given process can prove to be valuable. Our investigation into planarian heterotrimeric G protein subunits produced functionally distinct and measurable phenotypes, supporting the idea that planarian heterotrimeric G protein subunits could provide a practical first step for identifying and studying roles of GPCRs.

To develop a G protein subunit-driven candidate approach, we formulated a pipeline that identifies candidate GPCR genes using phenotypes from our work along with published single cell sequencing datasets (Fig. 2h; Supplementary Table 3) (Fincher et al. 2018; Plass et al. 2018; Swapna et al. 2018). Our work with $G\beta x2$ and qcr052 demonstrates the utility of characterizing heterotrimeric G proteins as a first step in identifying relevant GPCRs and understanding the cellular mechanism (Wise et al. 2004; Oh et al. 2006; Civelli et al. 2013; Ngo et al. 2016). In the future, we plan to apply this approach to identify candidate GPCRs that work with heterotrimeric G proteins to promote polarity establishment and successful regeneration. Identification of novel signaling pathways with key roles in regeneration will help us understand how information about injury is converted into cellular responses to coordinate and drive planarian regeneration.

Data availability

Planarians and plasmids are available upon request. The authors affirm the inclusion of all relevant data and all data required to confirm conclusions of the work are present in the figures, article, tables, and supplementary material associated with this manuscript. Supplementary material is available at the Genetics website. In situ hybridization data will also be shared at the Planarian Anatomy Gene Expression (PAGE) database.

Supplemental material available at GENETICS online.

Acknowledgments

We thank Bidushi Chandra, Kendall Clay, Samantha Hack, Taylor Medlock-Lanier, and the reviewers for feedback on this manuscript. We also thank Bidushi Chandra, Kendall Clay, Taylor Medlock-Lanier, and Britessia Smith for the technical support and helpful discussions. We thank Alejandro Sánchez Alvarado and Shane Merryman (Stowers Institute) for providing planarians and for instructions on recirculation system construction. We thank Muthugapatti Kandasamy at the UGA Biomedical Microscopy Core for support with fluorescent imaging. Finally, we thank White Oak Pastures (Bluffton, GA) for beef liver.

Funding

This work was funded by generous support from the University of Georgia, NSF (IOS-1942822), the McKnight Foundation, and the Alfred P. Sloan Foundation.

Conflicts of interest

None declared.

Literature cited

- Agata K, Soejima Y, Kato K, Kobayashi C, Umesono Y, Watanabe K. Structure of the planarian central nervous system (CNS) revealed by neuronal cell markers. Zoolog Sci. 1998;15(3):433-440. doi:10.
- Alvarado AS, Newmark PA, Robb SMC, Juste R. The Schmidtea mediterranea database as a molecular resource for studying platyhelminthes, stem cells and regeneration. Development. 2002;129(24): 5659-5665. doi:10.1242/dev.00167.
- Anantharaman V, Abhiman S, de Souza RF, Aravind L. Comparative genomics uncovers novel structural and functional features of the heterotrimeric GTPase signaling system. Gene. 2011;475(2): 63-78. doi:10.1016/j.gene.2010.12.001.
- Baguna J, Salo E, Auladell C. Regeneration and pattern formation in planarians. III. that neoblasts are totipotent stem cells and the cells. Development. 1989;107(1):77-86. doi:10.1242/dev.107.1.77.
- Bates CA, Meyer RL. Heterotrimeric G protein activation rapidly inhibits outgrowth of optic axons from adult and embryonic mouse,

- and goldfish retinal explants. Brain Res. 1996;714(1-2):65-75. doi:10.1016/0006-8993(95)01468-3.
- Brandl H, Moon H, Vila-Farré M, Liu S-Y, Henry I, Rink JC. Planminea mineable resource of planarian biology and biodiversity. Nucleic Acids Res. 2016;44(D1):D764-D773. doi:10.1093/nar/ gkv1148.
- Brock C, Schaefer M, Reusch HP, Czupalla C, Michalke M, Spicher K, Schultz G, Nürnberg B. Roles of GBy in membrane recruitment and activation of p110γ/p101 phosphoinositide 3-kinase γ. J Cell Biol. 2003;160(1):89-99. doi:10.1083/jcb.200210115.
- Burch ML, Osman N, Getachew R, Al-aryahi S, Poronnik P, Zheng W, Hill MA, Little PJ. G protein coupled receptor transactivation: extending the paradigm to include serine/threonine kinase receptors. Int J Biochem Cell Biol. 2012;44(5):722-727. doi:10.1016/j. biocel.2012.01.018.
- Cebrià F, Kudome T, Nakazawa M, Mineta K, Ikeo K, Gojobori T, Agata K. The expression of neural-specific genes reveals the structural and molecular complexity of the planarian central nervous system. Mech Dev. 2002;116(1-2):199-204. doi:10.1016/S0925-4773(02)00134-X.
- Cebrià F, Newmark PA. Planarian homologs of netrin and netrin receptor are required for proper regeneration of the central nervous system and the maintenance of nervous system architecture. Development. 2005;132(16):3691-3703. doi:10.1242/dev.01941.
- Chan JD, Agbedanu PN, Grab T, Zamanian M, Dosa PI, Day TA, Marchant JS. Ergot alkaloids (re)generate new leads as antiparasitics. PLoS Negl Trop Dis. 2015;9(9):e0004063. doi:10.1371/journal. pntd.0004063.
- Chan JD, Grab T, Marchant JS. Kinetic profiling an abundantly expressed planarian serotonergic GPCR identifies bromocriptine as a perdurant antagonist. Int J Parasitol Drugs Drug Resist. 2016;6(3):356-363. doi:10.1016/j.ijpddr.2016.06.002.
- Chen Z, Wells CD, Sternweis PC, Sprang SR. Structure of the rgRGS domain of p115RhoGEF. Nat Struct Biol. 2001;8(9):805-809. doi: 10.1038/nsb0901-805.
- Choi HY, Saha SK, Kim K, Kim S, Yang G-M, Kim B, Kim J-H, Cho S-G. G protein-coupled receptors in stem cell maintenance and somatic reprogramming to pluripotent or cancer stem cells. BMB Rep. 2015;48(2):68-80. doi:10.5483/BMBRep.2015.48.2.250.
- Civelli O, Reinscheid RK, Zhang Y, Wang Z, Fredriksson R, Schiöth HB. G protein-coupled receptor deorphanizations. Annu Rev Pharmacol Toxicol. 2013;53(1):127-146. doi:10.1146/annurevpharmtox-010611-134548.
- Cloutier JK, McMann CL, Oderberg IM, Reddien PW. Activin-2 is required for regeneration of polarity on the planarian anteriorposterior axis. PLoS Genet. 2021;17(3):e1009466. doi:10.1371/ journal.pgen.1009466.
- Coleman D, Berghuis A, Lee E, Linder M, Gilman A, Sprang SR. Structures of active conformations of Gi alpha 1 and the mechanism of GTP hydrolysis. Science. 1994;265(5177):1405-1412. doi:10. 1126/science.8073283.
- Collins JJ, Hou X, Romanova EV, Lambrus BG, Miller CM, Saberi A, Sweedler JV, Newmark PA. Genome-wide analyses reveal a role for peptide hormones in planarian germline development. PLoS Biol. 2010;8(10):e1000509. doi:10.1371/journal.pbio.1000509.
- Currie KW, Pearson BJ. Transcription factors lhx1/5-1 and pitx are required for the maintenance and regeneration of serotonergic neurons in planarians. Development. 2013;140(17):3577-3588. doi:10.1242/dev.098590.
- Dereeper A, Guignon V, Blanc G, Audic S, Buffet S, Chevenet F, Dufayard J-F, Guindon S, Lefort V, Lescot M, et al. Phylogeny.fr: robust phylogenetic analysis for the non-specialist. Nucleic Acids Res. 2008;36(Web Server):W465-W469. doi:10.1093/nar/gkn180.

- Doze VA, Perez DM. GPCRs in stem cell function. Prog Mol Biol Transl Sci. 2013;115:175–216. doi:10.1016/B978-0-12-394587-7.00005-1.
- Dupré DJ, Robitaille M, Rebois RV, Hébert TE. The role of Gβγ subunits in the organization, assembly, and function of GPCR signaling complexes. Annu Rev Pharmacol Toxicol. 2009:49(1):31-56. doi: 10.1146/annurev-pharmtox-061008-103038.
- Edgar RC. MUSCLE: multiple sequence alignment with high accuracy and high throughput. Nucleic Acids Res. 2004;32(5):1792-1797. doi:10.1093/nar/gkh340.
- Eisenhoffer GT, Kang H, Alvarado AS. Molecular analysis of stem cells and their descendants during cell turnover and regeneration in the planarian Schmidtea mediterranea. Cell Stem Cell. 2008;3(3): 327-339. doi:10.1016/j.stem.2008.07.002.
- El-Gebali S, Mistry J, Bateman A, Eddy SR, Luciani A, Potter SC, Qureshi M, Richardson LJ, Salazar GA, Smart A, et al. The Pfam protein families database in 2019. Nucleic Acids Res. 2019;47-(D1):D427-D432. doi:10.1093/nar/gky995.
- Fincher CT, Wurtzel O, de Hoog T, Kravarik KM, Reddien PW. Cell type transcriptome atlas for the planarian Schmidtea mediterranea. Science. 2018;360(6391):eaaq1736. doi:10.1126/science.aaq1736.
- Forsthoefel DJ, Waters FA, Newmark PA. Generation of cell typespecific monoclonal antibodies for the planarian and optimization of sample processing for immunolabeling. BMC Dev Biol. 2014;14(1):45. doi:10.1186/s12861-014-0045-6.
- Fredriksson R, Lagerström MC, Lundin L-G, Schiöth HB. The G-protein-coupled receptors in the human genome form five main families. Phylogenetic analysis, paralogon groups, and fingerprints. Mol Pharmacol. 2003;63(6):1256-1272. doi:10.1124/ mol.63.6.1256.
- Garland SL. Are GPCRs still a source of new targets? J Biomol Screen. 2013;18(9):947-966. doi:10.1177/1087057113498418.
- Gasteiger E, Gattiker A, Hoogland C, Ivanyi I, Appel RD, Bairoch A. ExPASy: the proteomics server for in-depth protein knowledge and analysis. Nucleic Acids Res. 2003;31(13):3784-3788. doi:10. 1093/nar/gkg563.
- Gaviño MA, Wenemoser D, Wang IE, Reddien PW. Tissue absence initiates regeneration through follistatin-mediated inhibition of activin signaling. Elife. 2013;2:e00247. doi:10.7554/eLife.00247.
- Glazer AM, Wilkinson AW, Backer CB, Lapan SW, Gutzman JH, Cheeseman IM, Reddien PW. The Zn finger protein Iguana impacts Hedgehog signaling by promoting ciliogenesis. Dev Biol. 2010;337(1):148-156. doi:10.1016/j.ydbio.2009.10.025.
- Guindon S, Dufayard J-F, Lefort V, Anisimova M, Hordijk W, Gascuel O. New algorithms and methods to estimate maximumlikelihood phylogenies: assessing the performance of PhyML 3.0. Syst Biol. 2010;59(3):307-321. doi:10.1093/sysbio/syg010.
- Guo H, Du X, Zhang Y, Wu J, Wang C, Li M, Hua X, Zhang XA, Yan J. Specific miRNA-G protein-coupled receptor networks regulate Sox9a/Sox9b activities to promote gonadal rejuvenation in zebrafish. Stem Cells. 2019;37(9):1189-1199. doi:10.1002/stem.
- Gurley KA, Rink JC, Alvarado AS. β-Catenin defines head versus tail identity during planarian regeneration and homeostasis. Science. 2008;319(5861):323-327. doi:10.1126/science.1150029.
- Hendzel MJ, Wei Y, Mancini MA, van Hooser A, Ranalli T, Brinkley BR, Bazett-Jones DP, Allis CD. Mitosis-specific phosphorylation of histone H3 initiates primarily within pericentromeric heterochromatin during G2 and spreads in an ordered fashion coincident with mitotic chromosome condensation. Chromosoma. 1997; 106(6):348-360. doi:10.1007/s004120050256.
- Hinck AP, Mueller TD, Springer TA. Structural biology and evolution of the TGF-β family. Cold Spring Harb Perspect Biol. 2016;8(12): a022103. doi:10.1101/cshperspect.a022103.

- Hopkins AL, Groom CR. The druggable genome. Nat Rev Drug Discov. 2002;1(9):727-730. doi:10.1038/nrd892.
- Iglesias M, Almuedo-Castillo M, Aboobaker AA, Saló E. Early planarian brain regeneration is independent of blastema polarity mediated by the Wnt/B-catenin pathway. Dev Biol. 2011;358(1): 68-78. doi:10.1016/j.ydbio.2011.07.013.
- Iglesias M, Gomez-Skarmeta JL, Saló E, Adell T. Silencing of Smed -β catenin1 generates radial-like hypercephalized planarians. Development. 2008;135(7):1215-1221. doi:10.1242/dev.020289.
- Inglese J, Koch W, Touhara K, Lefkowitz R. GBy interactions with PH domains and Ras-MAPK signaling pathways. Trends Biochem Sci. 1995;20(4):151-156. doi:10.1016/S0968-0004(00)88992-6.
- Jansen G, Thijssen KL, Werner P, van derHorst M, Hazendonk E, Plasterk RHA. The complete family of genes encoding G proteins of Caenorhabditis elegans. Nat Genet. 1999;21(4):414-419. doi:10.
- Jones DT, Reed RR. Golf: an olfactory neuron specific-G protein involved in odorant signal transduction. Science. 1989;244(4906): 790-795. doi:10.1126/science.2499043.
- Kakugawa S, Langton PF, Zebisch M, Howell SA, Chang T-H, Liu Y, Feizi T, Bineva G, O'Reilly N, Snijders AP, et al. Notum deacylates Wnt proteins to suppress signalling activity. Nature. 2015;519-(7542):187-192. doi:10.1038/nature14259.
- King RS, Newmark PA. In situ hybridization protocol for enhanced detection of gene expression in the planarian Schmidtea mediterranea. BMC Dev Biol. 2013;13(1):8. doi:10.1186/1471-213X-13-8.
- Kiseleva EV, Sidorova MV, Gorbacheva LR, Strukova SM. Peptide-agonist of protease-activated receptor (PAR 1), similar to activated protein C, promotes proliferation in keratinocytes and wound healing of epithelial layer. Biomeditsinskaya Khimiya. 2014;60(6):702-706. doi:10.18097/PBMC20146006702.
- Krishnan A, Almén MS, Fredriksson R, Schiöth HB. The origin of GPCRs: identification of mammalian like rhodopsin, adhesion, glutamate and frizzled GPCRs in fungi. PLoS One. 2012;7(1): e29817. doi:10.1371/journal.pone.0029817.
- Kuang S, Doran SA, Wilson RJA, Goss GG, Goldberg JI. Serotonergic sensory-motor neurons mediate a behavioral response to hypoxia in pond snail embryos. J Neurobiol. 2002;52(1):73-83. doi: 10.1002/neu.10071.
- Labbé RM, Irimia M, Currie KW, Lin A, Zhu SJ, Brown DDR, Ross EJ, Voisin V, Bader GD, Blencowe BJ, et al. A comparative transcriptomic analysis reveals conserved features of stem cell pluripotency in planarians and mammals. Stem Cells. 2012;30(8): 1734-1745. doi:10.1002/stem.1144.
- Lagerström MC, Schiöth HB. Structural diversity of G proteincoupled receptors and significance for drug discovery. Nat Rev Drug Discov. 2008;7(4):339-357. doi:10.1038/nrd2518.
- Langenhan T, Barr MM, Bruchas MR, Ewer J, Griffith LC, Maiellaro I, Taghert PH, White BH, Monk KR. Model organisms in G proteincoupled receptor research. Mol Pharmacol. 2015;88(3):596-603. doi:10.1124/mol.115.098764.
- Lapan SW, Reddien PW. Transcriptome analysis of the planarian eye identifies ovo as a specific regulator of eye regeneration. Cell Rep. 2012;2(2):294-307. doi:10.1016/j.celrep.2012.06.018.
- Li S, Yang C, Zhang L, Gao X, Wang X, Liu W, Wang Y, Jiang S, Wong YH, Zhang Y, et al. Promoting axon regeneration in the adult CNS by modulation of the melanopsin/GPCR signaling. Proc Natl Acad Sci USA. 2016;113(7):1937–1942. doi:10.1073/pnas.1523645113.
- Liu S-Y, Rink JC. Total RNA isolation from planarian tissues. Methods Mol Biol. 2018;1774:259-265. doi:10.1007/978-1-4939-7802-1_6.
- Longenecker KL, Lewis ME, Chikumi H, Gutkind JS, Derewenda ZS. Structure of the RGS-like domain from PDZ-RhoGEF. Structure. 2001;9(7):559-569. doi:10.1016/S0969-2126(01)00620-7.

- Lozano BC. The identification and the functional validation of eye development and regeneration genes in schmidtea mediterranea,
- Malpe MS, McSwain LF, Kudyba K, Ng CL, Nicholson J, Brady M, Qian Y, Choksi V, Hudson AG, Parrott BB, et al. G-protein signaling is required for increasing germline stem cell division frequency in response to mating in Drosophila males. Sci Rep. 2020;10(1):3888. doi:10.1038/s41598-020-60807-8
- März M, Seebeck F, Bartscherer K. A Pitx transcription factor controls the establishment and maintenance of the serotonergic lineage in planarians. Development. 2013;140(22):4499-4509. doi:10. 1242/dev.100081.
- Mitchell AL, Attwood TK, Babbitt PC, Blum M, Bork P, Bridge A, Brown SD, Chang H-Y, El-Gebali S, Fraser MI, et al. Interpro in 2019: improving coverage, classification and access to protein sequence annotations. Nucleic Acids Res. 2019;47(D1):D351-D360. doi:10. 1093/nar/gky1100.
- Mönck HJ, Jörg A, von Falkenhausen T, Tanke J, Wild B, Dormagen D, Piotrowski J, Winklmayr C, Bierbach D, Landgraf T. BioTracker: an open-source computer vision framework for visual animal tracking. arXiv:1803.07985, 2018. https://doi.org/10.48550/arXiv.1803.
- Nakamura T, Takio K, Eto Y, Shibai H, Titani K, Sugino H. Activin-binding protein from rat ovary is follistatin. Science. 1990;247(4944):836-838. doi:10.1126/science.2106159.
- Newmark PA, Sánchez Alvarado A. Bromodeoxyuridine specifically labels the regenerative stem cells of planarians. Dev Biol. 2000; 220(2):142-153. doi:10.1006/dbio.2000.9645.
- Ngo T, Kufareva I, Coleman JL, Graham RM, Abagyan R, Smith NJ. Identifying ligands at orphan GPCRs: current status using structure-based approaches. Br J Pharmacol. 2016;173(20): 2934-2951. doi:10.1111/bph.13452.
- O'Connor JT, Stevens AC, Shannon EK, Akbar FB, LaFever KS, Narayanan NP, Gailey CD, Hutson MS, Page-McCaw A. Proteolytic activation of growth-blocking peptides triggers calcium responses through the GPCR Mthl10 during epithelial wound detection. Dev Cell. 2021;56(15):2160-2175.e5. doi:10. 1016/j.devcel.2021.06.020.
- Oh DY, Kim K, Kwon HB, Seong JY. Cellular and molecular biology of orphan G protein-coupled receptors. Int Rev Cytol. 2006;252: 163-218. doi:10.1016/S0074-7696(06)52003-0.
- Okamoto K, Takeuchi K, Agata K. Neural projections in planarian brain revealed by fluorescent dye tracing. Zoolog Sci. 2005;22(5): 535-546. doi:10.2108/zsj.22.535.
- Oldham WM, Hamm HE. Heterotrimeric G protein activation by G-protein-coupled receptors. Nat Rev Mol Cell Biol. 2008;9(1): 60-71. doi:10.1038/nrm2299.
- Owlarn S, Bartscherer K. Go ahead, grow a head! A planarian's Guide to anterior regeneration. Regeneration. 2016;3(3):139-155. doi:10.
- Pascual-Carreras E, Sureda-Gómez M, Barrull-Mascaró R, Jordà N, Gelabert M, Coronel-Córdoba P, Saló E, Adell T. WNT-FRIZZLED-LRP5/6 signaling mediates posterior fate and proliferation during planarian regeneration. Genes (Basel). 2021; 12(1):101. doi:10.3390/genes12010101.
- Petersen CP, Reddien PW. Smed-β catenin-1 is required for anteroposterior blastema polarity in planarian regeneration. Science. 2008; 319(5861):327-330. doi:10.1126/science.1149943.
- Petersen CP, Reddien PW. Polarized notum activation at wounds inhibits Wnt function to promote planarian head regeneration. Science. 2011;332(6031):852-855. doi:10.1126/science.1202143.
- Pierce KL, Premont RT, Lefkowitz RJ. Seven-transmembrane receptors. Nat Rev Mol Cell Biol. 2002;3(9):639-650. doi:10.1038/nrm908.

- Plass M, Solana J, Wolf FA, Ayoub S, Misios A, Glažar P, Obermayer B, Theis FJ, Kocks C, Rajewsky N. Cell type atlas and lineage tree of a whole complex animal by single-cell transcriptomics. Science. 2018;360(6391):eaaq1723. doi:10.1126/science.aaq1723.
- Raz AA, Wurtzel O, Reddien PW, Planarian stem cells specify fate vet retain potency during the cell cycle. Cell Stem Cell. 2021;28(7): 1307-1322.e5. doi:10.1016/j.stem.2021.03.021.
- Reddien PW. The cellular and molecular basis for planarian regeneration. Cell. 2018;175(2):327-345. doi:10.1016/j.cell.2018.09.021.
- Reddien PW, Bermange AL, Kicza AM, Sánchez Alvarado A. BMP Signaling regulates the dorsal planarian midline and is needed for asymmetric regeneration. Development. 2007;134(22): 4043-4051. doi:10.1242/dev.007138.
- Reddien PW, Oviedo NJ, Jennings JR, Jenkin JC, Alvarado AS. SMEDWI-2 Is a PIWI-like protein that regulates planarian stem cells. Science. 2005;310(5752):1327-1330. doi:10.1126/science. 1116110
- Robert X, Gouet P. Deciphering key features in protein structures with the new ENDscript server. Nucleic Acids Res. 2014;42(W1): W320-W324. doi:10.1093/nar/gku316.
- Roberts-Galbraith RH, Brubacher JL, Newmark PA. A functional genomics screen in planarians reveals regulators of whole-brain regeneration. Elife. 2016;5:e17002. doi:10.7554/eLife.17002.
- Roberts-Galbraith RH, Newmark PA. Follistatin antagonizes activin signaling and acts with notum to direct planarian head regeneration. Proc Natl Acad Sci USA. 2013;110(4):1363-1368. doi:10. 1073/pnas.1214053110.
- Ross KG, Molinaro AM, Romero C, Dockter B, Cable KL, Gonzalez K, Zhang S, Collins E-MS, Pearson BJ, Zayas RM. Soxb1 activity regulates sensory neuron regeneration, maintenance, and function in planarians. Dev Cell. 2018;47(3):331-347.e5. doi:10.1016/j.devcel. 2018 10 014
- Ross KG, Omuro KC, Taylor MR, Munday RK, Hubert A, King RS, Zayas RM. Novel monoclonal antibodies to study tissue regeneration in planarians. BMC Dev Biol. 2015;15(1):2. doi:10.1186/s12861-014-0050-9.
- Rouhana L, Weiss JA, Forsthoefel DJ, Lee H, King RS, Inoue T, Shibata N, Agata K, Newmark PA. RNA Interference by feeding in vitrosynthesized double-stranded RNA to planarians: methodology and dynamics. Dev Dyn. 2013;242(6):718-730. doi:10.1002/dvdy.
- Rozanski A, Moon H, Brandl H, Martín-Durán JM, Grohme MA, Hüttner K, Bartscherer K, Henry I, Rink JC. Planmine 3.0-improvements to a mineable resource of flatworm biology and biodiversity. Nucleic Acids Res. 2019;47(D1):D812-D820. doi:10.1093/ nar/gkv1070.
- Rozen S, Skaletsky H. Primer3 on the WWW for general users and for biologist programmers. In: Bioinformatics Methods and Protocols. Totowa (NJ): Humana Press; 1999. p. 365-386.
- Saberi A, Jamal A, Beets I, Schoofs L, Newmark PA. GPCRs direct germline development and somatic gonad function in planarians. PLoS Biol. 2016;14(5):e1002457. doi:10.1371/journal.pbio.1002457.
- Schafer AE, Blaxall BC. G protein coupled receptor-mediated transactivation of extracellular proteases. J Cardiovasc Pharmacol. 2017;70(1):10-15. doi:10.1097/FJC.0000000000000475.
- Schindelin J, Arganda-Carreras I, Frise E, Kaynig V, Longair M, Pietzsch T, Preibisch S, Rueden C, Saalfeld S, Schmid B, et al. Fiji: an open-source platform for biological-image analysis. Nat Methods. 2012;9(7):676-682. doi:10.1038/nmeth.2019.
- Scimone ML, Lapan SW, Reddien PW. A forkhead transcription factor is wound-induced at the planarian midline and required for anterior pole regeneration. PLoS Genet. 2014;10(1):e1003999. doi: 10.1371/journal.pgen.1003999.

- Shimizu T, Hisamoto N. Factors regulating axon regeneration via JNK MAP kinase in Caenorhabditis elegans. J Biochem. 2020;167(5): 433-439. doi:10.1093/jb/mvaa020.
- Sievers F, Higgins DG. Clustal Omega. Curr Protoc Bioinformatics. 2014:48(1):3.13.1-3.13.16. doi:10.1002/0471250953.bi0313s48.
- Smrcka AV. G protein By subunits: central mediators of G proteincoupled receptor signaling. Cell Mol Life Sci. 2008;65(14): 2191-2214. doi:10.1007/s00018-008-8006-5.
- Snow BE, Krumins AM, Brothers GM, Lee S-F, Wall MA, Chung S, Mangion J, Arva S, Gilman AG, Siderovski DP. A G protein subunitlike domain shared between RGS11 and other RGS proteins specifies binding to G_{B5} subunits. Proc Natl Acad Sci USA. 1998;95(22): 13307-13312. doi:10.1073/pnas.95.22.13307.
- Swapna LS, Molinaro AM, Lindsay-Mosher N, Pearson BJ, Parkinson J. Comparative transcriptomic analyses and single-cell RNA sequencing of the freshwater planarian Schmidtea mediterranea identify major cell types and pathway conservation. Genome Biol. 2018;19(1):124. doi:10.1186/s13059-018-1498-x.
- Syrovatkina V, Alegre KO, Dey R, Huang X-Y. Regulation, signaling, and physiological functions of G-proteins. J Mol Biol. 2016;428-(19):3850-3868. doi:10.1016/j.jmb.2016.08.002.
- Tang W-J, Gilman AG. Type-specific regulation of adenylyl cyclase by G protein βy subunits. Science. 1991;254(5037):1500–1503. doi:10. 1126/science.1962211.
- Tewari AG, Stern SR, Oderberg IM, Reddien PW. Cellular and molecular responses unique to major injury are dispensable for planarian regeneration. Cell Rep. 2018;25(9):2577-2590.e3. doi:10.1016/j. celrep.2018.11.004.
- Tu KC, Cheng L-C, Vu H TK, Lange JJ, McKinney SA, Seidel CW, Sánchez Alvarado A. Egr-5 is a post-mitotic regulator of planarian epidermal differentiation. Elife. 2015;4:e10501. doi:10.7554/eLife.10501.
- Vogg MC, Owlarn S, Pérez Rico YA, Xie J, Suzuki Y, Gentile L, Wu W, Bartscherer K. Stem cell-dependent formation of a functional anterior regeneration pole in planarians requires Zic and Forkhead transcription factors. Dev Biol. 2014;390(2):136-148. doi:10.1016/j. ydbio.2014.03.016.
- Wagner DE, Wang IE, Reddien PW. Clonogenic neoblasts are pluripotent adult stem cells that underlie planarian regeneration. Science. 2011;332(6031):811-816. doi:10.1126/science.1203983.
- Wall MA, Coleman DE, Lee E, Iñiguez-Lluhi JA, Posner BA, Gilman AG, Sprang SR. The structure of the G protein heterotrimer Giα1β1γ2. Cell. 1995;83(6):1047-1058. doi:10.1016/0092-8674(95)90220-1.
- Wenemoser D, Lapan SW, Wilkinson AW, Bell GW, Reddien PW. A molecular wound response program associated with regeneration initiation in planarians. Genes Dev. 2012;26(9):988-1002. doi:10.1101/gad.187377.112.
- Wenemoser D, Reddien PW. Planarian regeneration involves distinct stem cell responses to wounds and tissue absence. Dev Biol. 2010; 344(2):979-991. doi:10.1016/j.ydbio.2010.06.017.

- Wise A, Gearing K, Rees S. Target validation of G-protein coupled receptors. Drug Discov Today. 2002;7(4):235-246. doi:10.1016/ S1359-6446(01)02131-6.
- Wise A, Jupe SC, Rees S. The identification of ligands at orphan G-protein coupled receptors. Annu Rev Pharmacol Toxicol. 2004; 44(1):43-66. doi:10.1146/annurev.pharmtox.44.101802.121419.
- Witchley JN, Mayer M, Wagner DE, Owen JH, Reddien PW. Muscle cells provide instructions for planarian regeneration. Cell Rep. 2013;4(4):633-641. doi:10.1016/j.celrep.2013.07.022.
- Wong GT, Gannon KS, Margolskee RF. Transduction of bitter and sweet taste by gustducin. Nature. 1996;381(6585):796-800. doi: 10.1038/381796a0.
- Wurtzel O, Cote LE, Poirier A, Satija R, Regev A, Reddien PW. A generic and cell-type-specific wound response precedes regeneration in planarians. Dev Cell. 2015;35(5):632-645. doi:10.1016/j.devcel. 2015.11.004.
- Yarfitz S, Hurley JB. Transduction mechanisms of vertebrate and invertebrate photoreceptors. J Biol Chem. 1994;269(20):14329--14332. doi:10.1016/S0021-9258(17)36620-6.
- Zamanian M. Genomic and functional characterization of G proteincoupled receptors in the human pathogen Schistosoma mansoni and the model planarian Schmidtea mediterranea. [Ames]: Iowa State University, Digital Repository, 2011.
- Zamanian M, Agbedanu PN, Wheeler NJ, McVeigh P, Kimber MJ, Day TA. Novel RNAi-mediated approach to G protein-coupled receptor deorphanization: proof of principle and characterization of a planarian 5-HT receptor. PLoS One. 2012;7(7):e40787. doi:10. 1371/journal.pone.0040787.
- Zamanian M, Kimber MJ, McVeigh P, Carlson SA, Maule AG, Day TA. The repertoire of G protein-coupled receptors in the human parasite Schistosoma mansoni and the model organism Schmidtea mediterranea. BMC Genomics. 2011;12(1):596. doi:10.1186/1471-2164-12-596
- Zeng A, Li H, Guo L, Gao X, McKinney S, Wang Y, Yu Z, Park J, Semerad C, Ross E, et al. Prospectively isolated tetraspanin+ neoblasts are adult pluripotent stem cells underlying planaria regeneration. Cell. 2018;173(7):1593-1608.e20. doi:10.1016/j.cell.2018. 05.006.
- Ziegler K, Kurz CL, Cypowyj S, Couillault C, Pophillat M, Pujol N, Ewbank JJ. Antifungal innate immunity in C. elegans: pKCδ links G protein signaling and a conserved p38 MAPK cascade. Cell Host Microbe. 2009;5(4):341-352. doi:10.1016/j.chom.2009.03.006.
- Zugasti O, Bose N, Squiban B, Belougne J, Kurz CL, Schroeder FC, Pujol N, Ewbank JJ. Activation of a G protein-coupled receptor by its endogenous ligand triggers the innate immune response of caenorhabditis elegans. Nat Immunol. 2014;15(9):833-838. doi:10.1038/ni.2957.

Editor: A. Sanchez Alvarado